Prediction, Smoothing and a Trilemma

Marc Wildi

February 29, 2024

Abstract

We propose a generic forecast approach, called Simple Sign Accuracy (SSA), which merges various facets of the prediction problem in terms of mean-square error, sign accuracy, zero crossings and smoothness. The latter is obtained in terms of a novel holding-time constraint which conditions the frequency of sign changes by the predictor. We obtain a solution to the optimization problem under fairly general assumptions, including a treatment of singular cases, and we derive the distribution of the predictor. In its simplest expression, our approach can be linked to smoothing and we compare the new zero-crossing constraint to a classic curvature penalty. Finally, we show that SSA sits on top of a generic prediction trilemma that addresses important user priorities, relevant to nowcasting and forecasting applications.

1 Introduction

Time series applications such as, e.g., forecasting or real-time signal extraction formalize attempts to educe information that is not yet readily available or accessible, from present and past data. Typically, optimality concepts rely on prediction accuracy or, more precisely, on the minimization of a distance measure between a target, for example a future observation or a (future or current) trend component, and the predictor. While this proceeding seems uncontroversial, in principle, we argue that alternative characteristics of a predictor might draw attention such as the smoothing capability, i.e., the extent by which undesirable 'noisy' components can be suppressed, or timeliness, as measured by lead, in terms of advancement or left-shift of a time series, or sign accuracy and zero-crossings, as measured by the ability to predict the correct sign of the target. We here propose a generic forecast approach which, under suitable assumptions, merges sign accuracy and mean-square error (MSE) performances subject to a holding time constraint which determines the expected number of zero-crossings of the predictor in a fixed time interval. McElroy Wildi (2019) propose an alternative methodological framework for addressing specific facets of the forecast problem but their approach does not accommodate for zero-crossings explicitly which may be viewed as a shortcoming in some applications.

Rice (1944) pioneered the analysis of zero-crossings by deriving a link between the autocorrelation function (ACF) of a zero-mean stationary Gaussian process and its expected number of crossings in a fixed time interval. Interestingly, sign changes of successively differenced processes can be informative about the entire autocorrelation sequence and thus the spectrum of a stationary time series, see Kedem (1986). A theoretical overview is provided by Kratz (2006). Applications have been proposed in the field of exploratory and inferential statistics, see Kedem (1986) and Barnett (1996) and are numerous in electronics and image processing, process discrimination, or pattern detection in speech, music, or radar screening. However, while most applications concern the analysis of current or past events, we here emphasize mainly a prospective prediction perspective.

In addition to being a self-contained and original prediction approach, SSA can address smoothness, either in a generic form or by customization of a specific benchmark. In the first case, we

compare the simplest expression of the SSA criterion with the Whittaker-Henderson approach, Whittaker (1922) and Henderson (1924), and we quantify performances based on the classic curvature measure as well as on the novel zero crossing rate; in the second case, we plug SSA on an existing benchmark predictor to modify some of its characteristics, addressing specifically timeliness, smoothness or MSE performances. We show that these three terms constitute a prediction trilemma on top of which SSA can trigger research priorities using suitable hyperparameter settings. Wildi (2024) proposes an application of SSA to a real-time business-cycle analysis, but the chosen treatment remains largely informal. We here fill this gap by providing complete theoretical results, including regular, singular and boundary cases; we also discuss numerical aspects and we propose a closed-form solution under certain assumptions; finally, we derive the sample distribution as well as a dual interpretation of the predictor. All empirical examples can be replicated in an open source SSA-package[1]. The proposed forecast approach is generic and can be extended to alternative signal specifications, predictors or data, for any forecast or backcast horizons: for illustration, in addition to the Hodrick and Prescott (1997) HP filter, the SSA package proposes applications to Hamilton's regression filter, Hamilton (2018), and to the Baxter-King (BK) band-pass filter, Baxter and King (1999).

Section (2) introduces the SSA criterion, relying on a basic methodological framework; a solution to the criterion is proposed in Section (3) together with accompanying technical results, including a derivation of the sample distribution; Section (4) provides background for a better interpretation of the SSA predictor; Section (5) proposes applications to time series forecasting and real-time signal extraction, highlighting a prediction trilemma whose constituents can be controlled by SSA; an extension of the basic framework to autocorrelated 'input' data is proposed in Section (6), allowing for exact finite sample results and zero-bias constraints in the case of non-stationary integrated processes; smoothing is addressed in Section (7) and Section (8) concludes by summarizing our main findings.

2 Simple Sign-Accuracy (SSA-) Criterion

Let $z_t = \sum_{k=-\infty}^{\infty} \gamma_k \epsilon_{t-k}$, where $\epsilon_j, j \in \mathbb{Z}$, is white noise which, for simplicity of exposition, is assumed to be standardized, and $\boldsymbol{\gamma} := (\gamma_k), k \in \mathbb{Z}$, is a (real) square summable sequence so that z_t is a stationary zero-mean process with variance $\sum_{k=-\infty}^{\infty} \gamma_k^2$. We look for a predictor $y_t := \sum_{k=0}^{L-1} b_k \epsilon_{t-k}$ of the target $z_{t+\delta}$, $\delta \in \mathbb{Z}$, where b_k are the coefficients of a one-sided causal filter of length L. This problem is commonly referred to as fore-, now- or backcast, depending on $\delta > 0$, $\delta = 0$ or $\delta < 0$, respectively. Consider the following optimization problem

$$
\left.
\begin{array}{c}
\max_{\mathbf{b}} \mathbf{b}' \boldsymbol{\gamma}_\delta \\
\mathbf{b}' \mathbf{M} \mathbf{b} = l\rho_1 \\
\mathbf{b}' \mathbf{b} = l
\end{array}
\right\},
\tag{1}
$$

where $\mathbf{b} = (b_0, ..., b_{L-1})$, $\boldsymbol{\gamma}_\delta = (\gamma_\delta, ..., \gamma_{\delta+L-1})'$ are L-dim. column vectors,

$$
\mathbf{M} = \left(
\begin{array}{ccccccccc}
0 & 0.5 & 0 & 0 & 0 & ... & 0 & 0 & 0 \\
0.5 & 0 & 0.5 & 0 & 0 & ... & 0 & 0 & 0 \\
... & & & & & & & & \\
0 & 0 & 0 & 0 & 0 & ... & 0.5 & 0 & 0.5 \\
0 & 0 & 0 & 0 & 0 & ... & 0 & 0.5 & 0
\end{array}
\right)
$$

is of dimension $L \cdot L$ and l is an arbitrary scaling. Criterion (1) is referred to as *simple sign accuracy* or SSA criterion, its solution is denoted by $SSA(\rho_1, \delta)$; the constraints $\mathbf{b}' \mathbf{M} \mathbf{b} = l\rho_1$ and $\mathbf{b}' \mathbf{b} = l$ are referred to as holding time (ht) and length constraints, respectively, see Wildi (2024). To simplify terminology, we now merge the concepts of filter outputs and filter weights such that,

---

[1] An R-package together with instructions, practical use-cases and theoretical results are to be found at https://github.com/wiaidp/R-package-SSA-Predictor.git.

e.g., $y_{t,MSE} := \boldsymbol{\gamma}_\delta' \boldsymbol{\epsilon}_t$ or $\boldsymbol{\gamma}_\delta$ will both be referred to as MSE predictor and similarly $y_t = \mathbf{b}\boldsymbol{\epsilon}_t$ or $\mathbf{b}$ are the SSA predictor, where $\boldsymbol{\epsilon}_t := (\epsilon_t, ..., \epsilon_{t-(L-1)})'$. The MSE-predictor $\boldsymbol{\gamma}_\delta$ stands for the proper target $\boldsymbol{\gamma}$ in Criterion (1) and we now assume $\boldsymbol{\gamma}_\delta \neq \mathbf{0}$: $\mathbf{b}$ (or $y_t := \mathbf{b}\boldsymbol{\epsilon}_t$) can be interpreted as a (constrained) predictor for $z_{t+\delta}$, see Section (5); alternatively, $\mathbf{b}$ can be viewed as a 'smoother' for $\boldsymbol{\gamma}_\delta$, see Section (7); in this sense, the SSA criterion merges prediction and smoothing and the particular objective function can retain pertinence outside of a classic prediction or MSE paradigm. Also, $\mathbf{b}'\mathbf{M}\mathbf{b}/l = \mathbf{b}'\mathbf{M}\mathbf{b}/\mathbf{b}'\mathbf{b} =: \rho(y,y,1)$ is the lag-one autocorrelation (ACF) of y_t and the objective function $\mathbf{b}'\boldsymbol{\gamma}_\delta$ is proportional to $\rho(y,z,\delta) := \mathbf{b}'\boldsymbol{\gamma}_\delta/\sqrt{l\boldsymbol{\gamma}'\boldsymbol{\gamma}}$, the target correlation of y_t with $z_{t+\delta}$, or to $\mathbf{b}'\boldsymbol{\gamma}_\delta/\sqrt{l\boldsymbol{\gamma}_\delta'\boldsymbol{\gamma}_\delta}$, the correlation of y_t with $y_{t,MSE}$: maximizing either of these objective functions maximizes the other ones, too and therefore Criterion (1) is equivalent to

$$\left.\begin{array}{c} \max_{\mathbf{b}} \rho(y,z,\delta) \\ \rho(y,y,1) = \rho_1 \\ \mathbf{b}'\mathbf{b} = l \end{array}\right\}. \tag{2}$$

If the holding time constraint $\rho(y,y,1) = \rho_1$ is omitted, then the solution to the SSA criterion is $\sqrt{l}\boldsymbol{\gamma}_\delta/\sqrt{\boldsymbol{\gamma}_\delta'\boldsymbol{\gamma}_\delta}$, thus replicating the MSE predictor up to an arbitrary scaling. As we shall see, the holding time constraint has an intuitively appealing interpretation that refers to a relevant problem in applications. An extension of the above basic framework to $\tilde{z}_t = \sum_{k=-\infty}^{\infty} \gamma_k x_{t-k}$, where x_t is an autocorrelated process, is proposed in Section (6) but we now first derive a solution to Criterion (1).

3 Solution to the SSA-Criterion

The eigenvectors $\mathbf{v}_j$ of $\mathbf{M}$ are the Fourier vectors $\mathbf{v}_j = \left(\sin(k\omega_j)/\sqrt{\sum_{k=1}^{L} sin(k\omega_j)^2}\right)_{k=1,...,L}$ with adjoined eigenvalues $\lambda_j = \cos(\omega_j)$ computed at the discrete Fourier frequencies $\omega_j = j\pi/(L+1)$, $j = 1,...,L$, see Anderson (1975): we normalize the eigenvectors to constitute an orthonormal basis of $\mathbb{R}^L$, which will simplify subsequent notation.

Proposition 1. *Under the above assumptions, the vector $\mathbf{b}$ is a stationary point of the lag-one ACF $\rho(y,y,1)$ if and only if $\mathbf{b}$ is an eigenvector $\mathbf{v}_i$ of $\mathbf{M}$ with corresponding eigenvalue $\lambda_i = \rho(y,y,1)$, for some $i \in \{1,...,L\}$. Furthermore, the lag-one ACF of a MA-filter of length L is bounded by $\lambda_L = -\cos(\pi/(L+1)) = \rho_{min}(L) \le \rho(y,y,1) \le \rho_{max}(L) = \cos(\pi/(L+1)) = \lambda_1$. Maximum and minimum ACF values are achieved for $\mathbf{b} := \mathbf{v}_1$ and $\mathbf{b} := \mathbf{v}_L$, respectively.*

Proof: Assume, for simplicity of exposition, that $\mathbf{b}'\mathbf{b} = 1$ so that $\rho(y,y,1) = \mathbf{b}'\mathbf{M}\mathbf{b}$. A stationary point of $\rho(y,y,1)$ is found by equating the derivative of the Lagrangian $\mathfrak{L} = \mathbf{b}'\mathbf{M}\mathbf{b} - \lambda(\mathbf{b}'\mathbf{b} - 1)$ to zero i.e. $(\mathbf{M} + \mathbf{M}')\mathbf{b} = 2\mathbf{M}\mathbf{b} = 2\lambda\mathbf{b}$. We deduce that $\mathbf{b}$ is a stationary point if and only if it is an eigenvector of $\mathbf{M}$. Then $\rho(y,y,1) = \mathbf{b}'\mathbf{M}\mathbf{b} = \lambda_i\mathbf{b}'\mathbf{b} = \lambda_i$ for some $i \in \{1,...,L\}$ and therefore $\rho(y,y,1)$ must be the corresponding eigenvalue, as claimed. Since the unit-sphere is free of boundary-points, we conclude that the extremal values $\rho_{min}(L), \rho_{max}(L)$ must be stationary points so that $\rho_{min}(L) = -\cos(\pi/(L+1)) = \lambda_L$ and $\rho_{max}(L) = \cos(\pi/(L+1)) = \lambda_1$ and the boundary values are reached by $\mathbf{b} := \mathbf{v}_L$ and $\mathbf{b} := \mathbf{v}_1$, respectively, as claimed. $\qquad\square$

We now introduce the spectral decomposition of the MSE-filter $\boldsymbol{\gamma}_\delta \neq \mathbf{0}$:

$$\boldsymbol{\gamma}_\delta = \sum_{i=n}^{m} w_i \mathbf{v}_i = \mathbf{V}\mathbf{w} \tag{3}$$

with (spectral-) weights $\mathbf{w} = (w_1, ..., w_L)'$, where $1 \le n \le m \le L$ and $w_m \neq 0, w_n \neq 0$. If $n > 1$ or $m < L$ then the MSE predictor $\boldsymbol{\gamma}_\delta$ is called *band-limited*. Also, we refer to $\boldsymbol{\gamma}_\delta$ as having either *complete* or *incomplete* spectral support depending on $w_i \neq 0$ for $i = 1,...,L$ or not. Finally, denote by $NZ := \{i|w_i \neq 0\}$ the set of indexes of non-vanishing weights w_i so that $NZ = \{1,2,...,L\}$ iff $\boldsymbol{\gamma}_\delta$ has complete spectral support in which case it is not band-limited.

3

Corollary 1. *Consider the SSA Criterion (1) and assume $\boldsymbol{\gamma}_\delta$ is not band-limited. If $\rho_1 < \lambda_L$ or $\rho_1 > \lambda_1$ then the problem does not admit a solution. For $\rho_1 = \lambda_1$ or $\rho_1 = \lambda_L$ the SSA solutions are $\mathbf{b}_1 := sign(w_1)\mathbf{v}_1$ and $\mathbf{b}_L := sign(w_L)\mathbf{v}_L$, respectively.*

A proof follows directly from Proposition (1), noting that $\mathbf{b}_1'\boldsymbol{\gamma}_\delta = sign(w_1)w_1 > 0$ and $\mathbf{b}_L'\boldsymbol{\gamma}_\delta = sign(w_L)w_L > 0$, where strict positiveness applies due to maximization and because $\boldsymbol{\gamma}_\delta$ is not band-limited.

Theorem 1. *Consider the SSA Criterion (1) and assume that the following set of regularity assumptions hold:*

1. *$\boldsymbol{\gamma}_\delta \neq 0$ (identifiability) and $L \geq 3$;*

2. *the SSA estimate $\mathbf{b}$ is not proportional to $\boldsymbol{\gamma}_\delta$, denoted by $\mathbf{b} \not\propto \boldsymbol{\gamma}_\delta$ (non-degenerate case);*

3. *$|\rho_1| < \rho_{max}(L)$ (admissibility);*

4. *the MSE-estimate $\boldsymbol{\gamma}_\delta$ has complete spectral support (completeness).*

Then:

1. *The solution to Criterion (1) has the one-parametric form*

$$\mathbf{b}(\nu) = D(\nu, l)\boldsymbol{\nu}^{-1}\boldsymbol{\gamma}_\delta = D(\nu, l) \sum_{i=1}^{L} \frac{w_i}{2\lambda_i - \nu} \mathbf{v}_i \tag{4}$$

   where $\nu \in \mathbb{R} \setminus \{2\lambda_i | i = 1, ..., L\}$, $D = D(\nu, l) \neq 0$ and $\boldsymbol{\nu} := 2\mathbf{M} - \nu\mathbf{I}$ is an invertible $L \cdot L$ matrix. Although $b_{-1}(\nu), b_L(\nu)$ do not explicitly appear in $\mathbf{b}(\nu)$ it is at least implicitly assumed that $b_{-1}(\nu) = b_L(\nu) = 0$ (implicit boundary constraints). Also, $D(\nu, l)$ is determined by ν and the length constraint; in particular, its sign is determined by asking for a positive objective function.

2. *The lag-one ACF of $y_t(\nu)$, where $y_t(\nu)$ denotes the output of $\mathbf{b}(\nu)$, is*

$$\rho(\nu) := \rho(y(\nu), y(\nu), 1) = \frac{\mathbf{b}(\nu)'\mathbf{M}\mathbf{b}(\nu)}{\mathbf{b}(\nu)'\mathbf{b}(\nu)} = \frac{\sum_{i=1}^{L} \lambda_i w_i^2 \frac{1}{(2\lambda_i - \nu)^2}}{\sum_{i=1}^{L} w_i^2 \frac{1}{(2\lambda_i - \nu)^2}} \tag{5}$$

   Moreover, $\nu = \nu(\rho_1)$ can always be found such that $y_t(\nu(\rho_1))$ complies with the holding-time constraint.

3. *The derivative $d\rho(\nu)/d\nu$ is strictly negative for $\nu \in \{x | |x| > 2\rho_{max}(L)\}$. Moreover, $max_{\nu < -2\rho_{max}(L)}\rho(\nu) = min_{\nu > 2\rho_{max}(L)}\rho(\nu) = \rho_{MSE}$, where ρ_{MSE} denotes the lag-one ACF of $\boldsymbol{\gamma}_\delta$.*

4. *For $\nu \in \{x | |x| > 2\rho_{max}(L)\}$ the derivatives of the objective function and lag-one ACF (with respect to ν) are linked by*

$$-sign(\nu)\frac{d\rho(y(\nu), z, \delta)}{d\nu} = \frac{1}{\left(\boldsymbol{\gamma}_\delta'\boldsymbol{\nu}^{-1}{}'\boldsymbol{\nu}^{-1}\boldsymbol{\gamma}_\delta\right)^{3/2}\sqrt{\boldsymbol{\gamma}_\delta'\boldsymbol{\gamma}_\delta}}\frac{d\rho(\nu)}{d\nu} < 0 \tag{6}$$

Proof: Define the Lagrangian $\mathcal{L} := \boldsymbol{\gamma}_\delta'\mathbf{b} - \tilde{\lambda}_1(\mathbf{b}'\mathbf{b} - 1) - \tilde{\lambda}_2(\mathbf{b}'\mathbf{M}\mathbf{b} - \rho_1)$, where we assume $l = 1$ in Criterion (1). By assumption, $L \geq 3$ so that $\mathbf{b}$ is defined on a $L - 2 \geq 1$ dimensional intersection of unit-sphere and holding-time hyperbola that is free of boundary points, see the appendix for details. Therefore, the solution $\mathbf{b}$ of the SSA problem must be a solution to the stationary Lagrangian equation

$$\boldsymbol{\gamma}_\delta = \tilde{\lambda}_1 2\mathbf{b} + \tilde{\lambda}_2(\mathbf{M} + \mathbf{M}')\mathbf{b} = \tilde{\lambda}_1 2\mathbf{b} + \tilde{\lambda}_2 2\mathbf{M}\mathbf{b}. \tag{7}$$

4

Since $\tilde{\lambda}_2 \neq 0$ (non-degenerate case) we obtain

$$D\boldsymbol{\gamma}_\delta \;=\; \boldsymbol{\nu}\mathbf{b}, \tag{8}$$

where $\boldsymbol{\nu} := (2\mathbf{M} - \nu\mathbf{I})$, $D = 1/\tilde{\lambda}_2 \neq 0^2$ and $\nu = -2\frac{\tilde{\lambda}_1}{\tilde{\lambda}_2}$. Furthermore, Equation (8) can be written in terms of a difference equation

$$b_{k+1} - \nu b_k + b_{k-1} \;=\; D\gamma_{k+\delta} \; , \; 0 \leq k \leq L-1, \tag{9}$$

assuming $b_{-1} = b_L = 0$. The eigenvalues of $\boldsymbol{\nu}$ are $2\lambda_i - \nu$ with corresponding eigenvectors $\mathbf{v}_i$. If $\mathbf{b}(\nu)$ is the solution to the SSA problem, then $\nu/2$ cannot be an eigenvalue of $\mathbf{M}$ since otherwise $\boldsymbol{\nu}$ in Equation (8) would map one of the eigenvectors to zero which would contradict the last regularity assumption, noting that $D \neq 0$. Therefore, $\nu \in \mathbb{R} \setminus \{2\lambda_i | i = 1, ..., L\}$, $\boldsymbol{\nu}^{-1}$ exists and $\boldsymbol{\nu}^{-1} = \mathbf{V}\mathbf{D}_\nu^{-1}\mathbf{V}'$, where the diagonal matrix $\mathbf{D}_\nu^{-1}$ has entries $\frac{1}{2\lambda_i - \nu}$. Solving for $\mathbf{b}$ in Equation (8) gives

$$\mathbf{b} \;=\; D\boldsymbol{\nu}^{-1}\boldsymbol{\gamma}_\delta \tag{10}$$

$$=\; D\mathbf{V}\mathbf{D}_\nu^{-1}\mathbf{V}'\mathbf{V}\mathbf{w}$$

$$=\; D\sum_{i=1}^{L} \frac{w_i}{2\lambda_i - \nu}\mathbf{v}_i. \tag{11}$$

as claimed. For a proof of Assertion (2) we look at

$$\rho(\nu) = \frac{\mathbf{b}'\mathbf{M}\mathbf{b}}{\mathbf{b}'\mathbf{b}} = \frac{\left(D\sum_{i=1}^{L}\frac{w_i}{2\lambda_i-\nu}\mathbf{v}_i\right)'\mathbf{M}\left(D\sum_{i=1}^{L}\frac{w_i}{2\lambda_i-\nu}\mathbf{v}_i\right)}{\left(D\sum_{i=1}^{L}\frac{w_i}{2\lambda_i-\nu}\mathbf{v}_i\right)'\left(D\sum_{i=1}^{L}\frac{w_i}{2\lambda_i-\nu}\mathbf{v}_i\right)} = \frac{\sum_{i=1}^{L}\frac{\lambda_i w_i^2}{(2\lambda_i-\nu)^2}}{\sum_{i=1}^{L}\frac{w_i^2}{(2\lambda_i-\nu)^2}} \tag{12}$$

We infer that $\lim_{\nu \to 2\lambda_i} \rho(\nu) = \lambda_i$, $i = 1, ..., L$. Since $\lambda_L = -\rho_{max}(L)$ and $\lambda_1 = \rho_{max}(L)$, we conclude that the limits $\pm\rho_{max}(L)$ can be reached by $\rho(\nu)$. Continuity of $\rho(\nu)$ and the intermediate-value theorem then imply that any $\rho_1 \in]-\rho_{max}(L), \rho_{max}(L)[$ is admissible for the holding-time constraint (the boundary cases where discussed in Corollary (1)).

We now proceed to a proof of Assertion (3):

$$\frac{d\rho\Big(y(\nu), y(\nu), 1\Big)}{d\nu} \;=\; \frac{d}{d\nu}\left(\frac{\mathbf{b}'\mathbf{M}\mathbf{b}}{\mathbf{b}'\mathbf{b}}\right) = \frac{d}{d\nu}\left(\frac{\boldsymbol{\gamma}_\delta'\boldsymbol{\nu}^{-1}{}'\mathbf{M}\boldsymbol{\nu}^{-1}\boldsymbol{\gamma}_\delta}{\boldsymbol{\gamma}_\delta'\boldsymbol{\nu}^{-1}{}'\boldsymbol{\nu}^{-1}\boldsymbol{\gamma}_\delta}\right) = \frac{d}{d\nu}\left(\frac{\boldsymbol{\gamma}_\delta'\mathbf{M}\boldsymbol{\nu}^{-2}\boldsymbol{\gamma}_\delta}{\boldsymbol{\gamma}_\delta'\boldsymbol{\nu}^{-2}\boldsymbol{\gamma}_\delta}\right)$$

$$=\; \frac{2\boldsymbol{\gamma}_\delta'\mathbf{M}\boldsymbol{\nu}^{-3}\boldsymbol{\gamma}_\delta\mathbf{b}'\mathbf{b}/D - (2\mathbf{b}'\mathbf{M}\mathbf{b}/D)\boldsymbol{\gamma}_\delta'\boldsymbol{\nu}^{-3}\boldsymbol{\gamma}_\delta}{((\mathbf{b}'\mathbf{b})^2/D^2)}$$

$$=\; \frac{2\mathbf{b}'\mathbf{M}\boldsymbol{\nu}^{-1}\mathbf{b}\mathbf{b}'\mathbf{b}/D^2 - 2\mathbf{b}'\mathbf{M}\mathbf{b}\mathbf{b}'\boldsymbol{\nu}^{-1}\mathbf{b}/D^2}{\mathbf{b}'\mathbf{b}/D^2}$$

$$=\; 2\mathbf{b}'\mathbf{M}\boldsymbol{\nu}^{-1}\mathbf{b}\mathbf{b}'\mathbf{b} - 2\mathbf{b}'\mathbf{M}\mathbf{b}\mathbf{b}'\boldsymbol{\nu}^{-1}\mathbf{b} \tag{13}$$

where $\boldsymbol{\nu}^{-k} := (\boldsymbol{\nu}^{-1})^k$, $\boldsymbol{\nu}^{-1}{}' = \boldsymbol{\nu}^{-1}$ (symmetry); commutativity of the matrix multiplications (used in deriving the third and next-to-last equations) follows from the fact that the matrices are symmetric and simultaneously diagonalizable (same eigenvectors); also we relied on generic matrix differentiation rules in the third equation[3]; finally we relied on $\mathbf{b}'\mathbf{b} = 1$ in the last equation. We can now insert $\mathbf{M}\boldsymbol{\nu}^{-1} = \frac{\nu}{2}\boldsymbol{\nu}^{-1} + 0.5\mathbf{I}$, which is a reformulation of $(2\mathbf{M} - \nu\mathbf{I})\boldsymbol{\nu}^{-1} = \mathbf{I}$, into the first

---

[2]$\mathbf{b}$ is defined on a $L - 2 \geq 1$-dimensional space so that the objective function is not overruled by the constraint, i.e., $|\tilde{\lambda}_2| < \infty$.

[3]$\frac{d(\boldsymbol{\nu}^{-1})}{d\nu} = \boldsymbol{\nu}^{-2}$ and $\frac{d(\boldsymbol{\nu}^{-2})}{d\nu} = 2\boldsymbol{\nu}^{-3}$. For the first equation the general rule is $\frac{d(\boldsymbol{\nu}^{-1})}{d\nu} = -\boldsymbol{\nu}^{-1}\frac{d\boldsymbol{\nu}}{d\nu}\boldsymbol{\nu}^{-1}$, noting that $\frac{d\boldsymbol{\nu}}{d\nu} = -\mathbf{I}$. The second equation follows by inserting the first equation into $\frac{d(\boldsymbol{\nu}^{-2})}{d\nu} = \frac{d(\boldsymbol{\nu}^{-1})}{d\nu}\boldsymbol{\nu}^{-1} + \boldsymbol{\nu}^{-1}\frac{d(\boldsymbol{\nu}^{-1})}{d\nu}$.

summand in 13 to obtain $2\mathbf{b}'\mathbf{M}\boldsymbol{\nu}^{-1}\mathbf{b}\mathbf{b}'\mathbf{b} = \left(\nu\mathbf{b}'\boldsymbol{\nu}^{-1}\mathbf{b} + \mathbf{b}'\mathbf{b}\right)\mathbf{b}'\mathbf{b}$. Plugging this expression into 13 and isolating $\mathbf{b}'\boldsymbol{\nu}^{-1}\mathbf{b}$ gives

$$
\begin{aligned}
\frac{d\rho\Big(y(\nu), y(\nu), 1\Big)}{d\nu} &= -\mathbf{b}'\boldsymbol{\nu}^{-1}\mathbf{b}\left(2\mathbf{b}'\mathbf{M}\mathbf{b} - \nu\mathbf{b}'\mathbf{b}\right) + (\mathbf{b}'\mathbf{b})^2 \\
&= -\mathbf{b}'\boldsymbol{\nu}^{-1}\mathbf{b}\mathbf{b}'\left(2\mathbf{M} - \nu\mathbf{I}\right)\mathbf{b} + (\mathbf{b}'\mathbf{b})^2 \\
&= -\mathbf{b}'\boldsymbol{\nu}^{-1}\mathbf{b}\mathbf{b}'\nu\mathbf{b} + (\mathbf{b}'\mathbf{b})^2 \\
&= -\boldsymbol{\gamma}_\delta'\boldsymbol{\nu}^{-3}\boldsymbol{\gamma}_\delta\boldsymbol{\gamma}_\delta'\boldsymbol{\nu}^{-1}\boldsymbol{\gamma}_\delta + (\boldsymbol{\gamma}_\delta'\boldsymbol{\nu}^{-2}\boldsymbol{\gamma}_\delta)^2 \\
&= -\boldsymbol{\gamma}_\delta'\mathbf{V}\mathbf{D}^{-3}\mathbf{V}'\boldsymbol{\gamma}_\delta\boldsymbol{\gamma}_\delta'\mathbf{V}\mathbf{D}^{-1}\mathbf{V}'\boldsymbol{\gamma}_\delta + (\boldsymbol{\gamma}_\delta'\mathbf{V}\mathbf{D}^{-2}\mathbf{V}'\boldsymbol{\gamma}_\delta)^2 \\
&= -\mathbf{w}'\mathbf{D}^{-3}\mathbf{w}\mathbf{w}'\mathbf{D}^{-1}\mathbf{w} + (\mathbf{w}'\mathbf{D}^{-2}\mathbf{w})^2,
\end{aligned}
\tag{14}
$$

where $\boldsymbol{\nu}^{-k} = \mathbf{V}\mathbf{D}^{-k}\mathbf{V}'$ and $\mathbf{D}^{-k}$, $k = 1, 2, 3$, is diagonal with eigenvalues $\lambda_{i\nu}^{-k} := (2\lambda_i - \nu)^{-k}$: the eigenvalues are (strictly) positive, if $\nu < -2\rho_{max}(L)$; if $\nu > 2\rho_{max}(L)$ then the eigenvalues are (strictly) negative, if k is an odd number, or (strictly) positive, if k is an even number. We then conclude

$$
\begin{aligned}
\frac{d\rho\Big(y(\nu), y(\nu), 1\Big)}{d\nu} &= -\sum_{j=0}^{L-1} w_j^2 \lambda_{j\nu}^{-3} \sum_{j=0}^{L-1} w_j^2 \lambda_{j\nu}^{-1} + \left(\sum_{j=0}^{L-1} w_j^2 \lambda_{j\nu}^{-2}\right)^2 \\
&= -\sum_{i>k} w_i^2 w_k^2 \left(\lambda_{i\nu}^{-1}\lambda_{k\nu}^{-3} + \lambda_{i\nu}^{-3}\lambda_{k\nu}^{-1} - 2\lambda_{i\nu}^{-2}\lambda_{k\nu}^{-2}\right),
\end{aligned}
\tag{15}
$$

where the terms in w_j^4 cancel. Now

$$
\lambda_{i\nu}^{-1}\lambda_{k\nu}^{-3} + \lambda_{i\nu}^{-3}\lambda_{k\nu}^{-1} - 2\lambda_{i\nu}^{-2}\lambda_{k\nu}^{-2} = \lambda_{i\nu}^{-1}\lambda_{k\nu}^{-1}\left(\lambda_{i\nu}^{-2} + \lambda_{k\nu}^{-2} - 2\lambda_{i\nu}^{-1}\lambda_{k\nu}^{-1}\right) = \lambda_{i\nu}^{-1}\lambda_{k\nu}^{-1}\left(\lambda_{i\nu}^{-1} - \lambda_{k\nu}^{-1}\right)^2 > 0,
$$

where the strict inequality holds because $\lambda_{i\nu}^{-1} = (2\lambda_i - \nu)^{-1}$ are of the same sign, pairwise different and non-vanishing if $|\nu| > 2\rho_{max}(L)$. Since $w_i \neq 0$ (last regularity assumption: completeness) we deduce $w_i^2 w_k^2 \neq 0$ in 15. Therefore, the latter expression is strictly negative and we conclude that $\rho\Big(y(\nu), y(\nu), 1\Big)$ must be a strictly monotonic function of ν for $\nu \in \{x | x > 2\rho_{max}(L)\}$ or for $\nu \in \{x | x < -2\rho_{max}(L)\}$. From $\lim_{|\nu| \to \infty} \rho(\nu) = \frac{\sum_{i=1}^{L} \lambda_i w_i^2}{\sum_{i=1}^{L} w_i^2} = \rho_{MSE}$ and $\frac{d\rho(\nu)}{d\nu} < 0$ we then infer $\max_{\nu < -2\rho_{max}(L)}\rho(\nu) = \min_{\nu > 2\rho_{max}(L)}\rho(\nu) = \rho_{MSE}$.

For a proof of the last Assertion (4) we look at

$$
\rho(y(\nu), z, \delta) = \frac{\mathbf{b}'\boldsymbol{\gamma}_\delta}{\sqrt{\mathbf{b}'\mathbf{b}\boldsymbol{\gamma}_\delta'\boldsymbol{\gamma}_\delta}} = D\frac{\boldsymbol{\gamma}_\delta'\boldsymbol{\nu}^{-1}\boldsymbol{\gamma}_\delta}{\sqrt{D^2\boldsymbol{\gamma}_\delta'\boldsymbol{\nu}^{-2}\boldsymbol{\gamma}_\delta\boldsymbol{\gamma}_\delta'\boldsymbol{\gamma}_\delta}} = D\frac{\sum_{i=1}^{L} \frac{w_i}{2\lambda_i-\nu}\mathbf{v}_i' \sum_{j=1}^{L} w_j\mathbf{v}_j}{\sqrt{D^2\boldsymbol{\gamma}_\delta'\boldsymbol{\nu}^{-2}\boldsymbol{\gamma}_\delta\boldsymbol{\gamma}_\delta'\boldsymbol{\gamma}_\delta}} = \text{sign}(D)\frac{\sum_{i=1}^{L} \frac{w_i^2}{2\lambda_i-\nu}}{\sqrt{\boldsymbol{\gamma}_\delta'\boldsymbol{\nu}^{-2}\boldsymbol{\gamma}_\delta\boldsymbol{\gamma}_\delta'\boldsymbol{\gamma}_\delta}}
$$

For $\nu < -2\rho_{max}(L)$ the quotient is strictly positive and therefore positiveness of the objective function implies $\text{sign}(D) > 0$; for $\nu > 2\rho_{max}(L)$ the quotient is strictly negative so that $\text{sign}(D) <$

0. Assume now that $\nu < -2\rho_{max}(L)$ so that

$$
\begin{aligned}
\frac{d\rho\Big(y(\nu), z, \delta\Big)}{d\nu} &= \frac{d}{d\nu}\left(\frac{\gamma_\delta' \boldsymbol{\nu}^{-1}\gamma_\delta}{\sqrt{\gamma_\delta' \boldsymbol{\nu}^{-2}\gamma_\delta \gamma_\delta' \gamma_\delta}}\right) \\
&= \frac{\gamma_\delta' \boldsymbol{\nu}^{-2}\gamma_\delta}{\sqrt{\gamma_\delta' \boldsymbol{\nu}^{-2}\gamma_\delta \gamma_\delta' \gamma_\delta}} - \frac{\gamma_\delta' \boldsymbol{\nu}^{-1}\gamma_\delta \gamma_\delta' \boldsymbol{\nu}^{-3}\gamma_\delta \gamma_\delta' \gamma_\delta}{(\gamma_\delta' \boldsymbol{\nu}^{-2}\gamma_\delta \gamma_\delta' \gamma_\delta)^{3/2}} \\
&= \frac{\left(\gamma_\delta' \boldsymbol{\nu}^{-2}\gamma_\delta\right)^2 \gamma_\delta' \gamma_\delta}{(\gamma_\delta' \boldsymbol{\nu}^{-2}\gamma_\delta \gamma_\delta' \gamma_\delta)^{3/2}} - \frac{\gamma_\delta' \boldsymbol{\nu}^{-1}\gamma_\delta \gamma_\delta' \boldsymbol{\nu}^{-3}\gamma_\delta \gamma_\delta' \gamma_\delta}{(\gamma_\delta' \boldsymbol{\nu}^{-2}\gamma_\delta \gamma_\delta' \gamma_\delta)^{3/2}} \\
&= \frac{1}{(\gamma_\delta' \boldsymbol{\nu}^{-2}\gamma_\delta)^{3/2}\sqrt{\gamma_\delta' \gamma_\delta}}\left\{\left(\gamma_\delta' \boldsymbol{\nu}^{-2}\gamma_\delta\right)^2 - \gamma_\delta' \boldsymbol{\nu}^{-1}\gamma_\delta \gamma_\delta' \boldsymbol{\nu}^{-3}\gamma_\delta\right\} \\
&= \frac{1}{(\gamma_\delta' \boldsymbol{\nu}^{-2}\gamma_\delta)^{3/2}\sqrt{\gamma_\delta' \gamma_\delta}}\frac{d\rho\Big(y(\nu), y(\nu), 1\Big)}{d\nu} < 0
\end{aligned}
$$

The last equality is obtained by recognizing that the expression in curly brackets is the same as in Equation (14). The proof applies also to $\nu > 2\rho_{max}(L)$ but with a changed sign, $\text{sign}(D) = -1$, and accordingly modified strict inequality, as was to be shown. $\qquad\square$

Remarks: The theorem derives exact finite-length solutions for any L such that $3 \leq L \leq T-1$ and the best predictor is obtained for $L = T-1$ but the corresponding sample history would consist of a single point, thus rendering direct comparisons with a benchmark impossible. Also, Equations (4) and (9) correspond to frequency-domain and time-domain solutions whose peculiar structures will be exploited further down. Finally, Equation (6) formalizes a fundamental tradeoff or dilemma between the target correlation and the lag-one ACF for the solution of the SSA problem which will be addressed and quantified in some of our examples.

The case of incomplete spectral support, assuming violation of the last regularity assumption of Theorem (1), is addressed in the following corollary.

Corollary 2. *Let all regularity assumptions of Theorem (1) hold, except completeness.*

1. *If $\nu \in \mathbb{R} \setminus \{2\lambda_i | i = 1, ..., L\}$, then the SSA predictor becomes*

$$
\mathbf{b}(\nu) = D \sum_{i \in NZ} \frac{w_i}{2\lambda_i - \nu} \mathbf{v}_i \tag{16}
$$

   where $NZ \subset \{1, ..., L\}$. The lag-one ACF is

$$
\rho(\nu) = \frac{\sum_{i \in NZ} \frac{\lambda_i w_i^2}{(2\lambda_i - \nu)^2}}{\sum_{i \in NZ} \frac{w_i^2}{(2\lambda_i - \nu)^2}} =: \frac{M_1}{M_2} \tag{17}
$$

   where M_1, M_2 are identified with nominator and denominator in this expression.

2. *Let $\nu = \nu_{i_0} := 2\lambda_{i_0}$ where $i_0 \notin NZ$ with adjoined rank-defficient $\boldsymbol{\nu}_{i_0} = 2\mathbf{M} - \nu_{i_0}\mathbf{I}$. Consider $\mathbf{b}(\nu_{i_0})$, $\rho(\nu_{i_0})$ and $M_{i_0 1}, M_{i_0 2}$ as defined in the previous assertion. In this case, $\mathbf{b}(\nu_{i_0})$ can be 'spectrally completed' as in*

$$
\mathbf{b}_{i_0}(\tilde{N}_{i_0}) := \mathbf{b}(\nu_{i_0}) + D\tilde{N}_{i_0}\mathbf{v}_{i_0} \tag{18}
$$

   with lag-one ACF

$$
\rho_{i_0}(\tilde{N}_{i_0}) = \frac{M_{i_0 1} + \lambda_{i_0}\tilde{N}_{i_0}^2}{M_{i_0 2} + \tilde{N}_{i_0}^2} \tag{19}
$$

7

If i_0 is such that $0 < \rho(\nu_{i_0}) = \frac{M_{i_0 1}}{M_{i_0 2}} < \rho_1 < \lambda_{i_0}$ or $0 > \rho(\nu_{i_0}) = \frac{M_{i_0 1}}{M_{i_0 2}} > \rho_1 > \lambda_{i_0}$, then

$$\tilde{N}_{i_0} = \pm \sqrt{\frac{\rho_1 M_{i_0 2} - M_{i_0 1}}{\lambda_{i_0} - \rho_1}} \tag{20}$$

ensures compliance with the holding-time constraint, i.e., $\rho_{i_0}(\tilde{N}_{i_0}) = \rho_1$. The 'correct' sign-combination of D and $\tilde{N}_{i_0}$ is determined by the corresponding maximum of the SSA objective function.

3. *If $\boldsymbol{\gamma}_\delta$ is not band limited, then any ρ_1 such that $|\rho_1| \leq \rho_{max}(L)$ is admissible in the holding-time constraint; If $w_1 = 0, w_L \neq 0$ then any ρ_1 such that $-\rho_{max}(L) < \rho_1 \leq \rho_{max}(L)$ is admissible ; If $w_1 \neq 0, w_L = 0$ then any ρ_1 such that $-\rho_{max}(L) \leq \rho_1 < \rho_{max}(L)$ is admissible; finally, if $w_1 = w_L = 0$ then any ρ_1 such that $-\rho_{max}(L) < \rho_1 < \rho_{max}(L)$ is admissible*

A proof of the corollary and a worked-out example are provided in the appendix. We now propose a solution to the SSA problem.

Corollary 3. *Let the assumptions of theorem 1 hold. Then the solution to the SSA-optimization problem (1) is given by $s\mathbf{b}(\nu)$ where $\mathbf{b}(\nu)$ is obtained from Equation (4), assuming an arbitrary scaling $|D| = 1$ (the sign of D is determined by asking for a positive objective function), ν_1 is a solution to the non-linear equation $\rho(\nu_1) = \rho_1$ and where $s = \sqrt{l/\mathbf{b}'\mathbf{b}}$. If the search for an optimal ν can be restricted to $\nu \in \{x | |x| > 2\rho_{max}(L)\}$, then ν_1 is determined uniquely by ρ_1.*

A proof follows directly from Theorem (1), noting that the scaling $s = \sqrt{l/\mathbf{b}'\mathbf{b}}$ interferes neither with the objective function nor with the holding time constraint and can be set afterward, once a solution assuming an arbitrary scaling $|D| = 1$ has been obtained. In particular, Assertion (3) warrants uniqueness for $\nu \in \{x | |x| > 2\rho_{max}(L)\}$. $\qquad\square$

In addition to uniqueness, Assertion (3) also ensures swift numerical optimization[4]. In this context, we now propose an exact closed-form solution for ν_1 as a function of ρ_1 in the non-linear (holding time) equation $\rho(\nu_1) = \rho_1$, assuming a particular target specification.

Corollary 4. *Let the following assumptions hold in addition to the set of regularity conditions of theorem 1:*

1. *$\boldsymbol{\gamma}_\delta \propto (\lambda^k)_{k=0,...,L-1}$ with stable root $\lambda \neq 0$ (stationary AR(1));*

2. *$|\nu| > 2$ so that $\nu = \lambda_{\rho_1} + 1/\lambda_{\rho_1}$ where $\lambda_{\rho_1} \in]-1, 1[\setminus\{0\}$;*

3. *$\lambda \neq \lambda_{\rho_1}$ (non-singular case);*

4. *$\lambda_{\rho_1}, \lambda$ and L are such that $\max(|\lambda_{\rho_1}|^{2k}, |\lambda|^{2k})$ is negligible for $k > L$ (sufficiently fast decay for given L).*

Then the optimal λ_{ρ_1} is obtained as (the real-valued)

$$\lambda_{\rho_1} = -\frac{1}{3c_3}\left(c_2 + C + \frac{\Delta_0}{C}\right) \tag{21}$$

where

$$C = \sqrt[3]{\frac{\Delta_1 + \text{sign}(\Delta_1)\sqrt{\Delta_1^2 - 4\Delta_0^3}}{2}} \tag{22}$$

$$\Delta_0 = c_2^2 - 3c_3 c_1$$

$$\Delta_1 = 2c_2^3 - 9c_3 c_2 c_1 + 27c_3^2 c_0$$

---

[4]The optimal parameter can be obtained by triangulation, in intervals of exponentially decaying width of order $1/2^n$, where n is the number of iteration steps.

and where c_3, c_2, c_1, c_0 are the coefficients of a cubic polynomial which depend on the AR(1)-target specified by λ and the holding-time constraint ρ_1 according to

$$c_3 = \lambda^{-2} - \rho_1 \lambda^{-1} \ , \ c_2 = -\lambda^{-1} - \rho_1(\lambda^{-2} - 2) \ , \ c_1 = -1 - \rho_1(\lambda - 2\lambda^{-1}) \ , \ c_0 = \lambda - \rho_1$$

The SSA predictor $\mathbf{b}(\nu_1) = \mathbf{b}(\lambda_{\rho_1} + 1/\lambda_{\rho_1})$ is then uniquely determined in closed-form by 4, down to a proper scaling, ensuring compliance with the length constraint, and the correct sign, leading to a positive criterion value $\mathbf{b}(\nu_1)' \boldsymbol{\gamma}_\delta > 0$.

A proof of the corollary makes use of the difference Equation (9) and can be found in the appendix. Note that a a closed-form expression in the case of an AR(p) target with $p > 1$ does generally not exist, see the appendix for reference. We now address the distribution of the SSA predictor.

Corollary 5. *Let all regularity assumptions of theorem 1 hold and let $\hat{\boldsymbol{\gamma}}_\delta$ be a finite-sample estimate of the MSE-predictor $\boldsymbol{\gamma}_\delta$ with mean $\boldsymbol{\mu}_{\gamma_\delta}$ and variance $\boldsymbol{\Sigma}_{\gamma_\delta}$. Then mean and variance of the SSA predictor $\hat{\mathbf{b}}(\nu)$ are*

$$\begin{aligned} \boldsymbol{\mu}_{\mathbf{b}} &= D\boldsymbol{\nu}^{-1}\boldsymbol{\mu}_{\gamma_\delta} \\ \boldsymbol{\Sigma}_{\mathbf{b}} &= D^2\boldsymbol{\nu}^{-1}\boldsymbol{\Sigma}_{\gamma_\delta}\boldsymbol{\nu}^{-1} \end{aligned}$$

If $\hat{\boldsymbol{\gamma}}_\delta$ is Gaussian distributed then so is $\hat{\mathbf{b}}(\nu)$.

The proof follows directly from Equation 4 and we refer to standard textbooks for a derivation of mean, variance and (asymptotic) distribution of the MSE-estimate under various assumptions about x_t, see Brockwell and Davis (1993). Our last result in this section proposes a dual interpretation of the SSA predictor.

Corollary 6. *Let all regularity assumptions of Theorem (1) hold and let $y_t(\nu_1)$ denote the SSA-solution for some $\nu_1 > 2\rho_{max}(L)$. Set $\rho_{\nu_1,\delta} := \rho(y(\nu_1), z, \delta)$ and consider the dual optimization problem*

$$\left. \begin{aligned} &\max_{\mathbf{b}} \rho(y, y, 1) \\ &\rho(y, z, \delta) = \rho_{\nu_1,\delta} \end{aligned} \right\} \tag{23}$$

The solution to this criterion has the same functional form as the original SSA problem and if the search for an optimal ν can be restricted to the set $\{\nu | |\nu| > 2\rho_{max}(L)\}$ then $y_t(\nu_1)$ is also the solution to the dual problem. If $\nu_1 < -2\rho_{max}(L)$, then $y_t(\nu_1)$ is the solution to the dual problem if minimization is substituted for maximization in the objective of Criterion (23).

Proof: Let us first examine the case $\nu_1 > 2\rho_{max}(l)$. The Lagrangian Equation (7) does not discern constraint and objective: after suitable re-scaling of multipliers, the problem specified by Criterion (23) leads to the same functional form $\mathbf{b} = D\boldsymbol{\nu}^{-1}\boldsymbol{\gamma}_\delta$ of its solution[5]. The only difference is that ν in Criterion (23) must be selected such that $\rho(y(\nu), z, \delta) = \rho_{\nu_1,\delta}$. If the search can be restricted to $\nu \in \{x | x > 2\rho_{max}(L)\}$, then by Assertion (4) the solution to the primal problem is also a solution to the dual problem, due to strict monotonicity of $\rho(y(\nu), z, \delta)$. The extension to $\nu \in \{x | |x| > 2\rho_{max}(L)\}$ follows from Assertion (3) which affirms that $\rho(\nu) < \rho(\nu_1)$ if $\nu < -2\rho_{max}(L)$. Similar reasoning applies if $\nu_1 < -2\rho_{max}(L)$, noting that maximization must be replaced by minimization in the dual Criterion (23) (because $\rho(\nu) > \rho(\nu_1)$ if $\nu > 2\rho_{max}(L)$). $\square$

We now interpret the obtained SSA solution and we shall see that the restriction $|\nu| > 2\rho_{max}(L)$ in the previous Corollaries (3), (4) and (6) is not a limitation since in applications, typically the more stringent condition $|\nu| > 2$ (most often $\nu > 2$) applies.

---

[5]Re-scaling is always possible because the regularity assumptions imply non-vanishing and finitely-sized multipliers.

4 Interpretation

4.1 Frequency-Domain Analysis and an Application To Real-Time Signal Extraction

Formally, the SSA-AR(2) filter (SSA-AR(2) for short) in the difference Equation (9) has transfer function $\Gamma_{AR(2)}(\nu, \omega) = \frac{1}{\exp(-i\omega) - \nu + \exp(i\omega)} = \frac{1}{2\cos(\omega) - \nu}$. Let then $\mathbf{\Gamma}_{AR(2)}(\nu)$ denote the vector of transfer function ordinates of SSA-AR(2) evaluated at the Fourier frequencies $\omega_j = j\pi/(L+1)$, $j = 1, ..., L$. Equation (11) implies

$$\mathbf{b}(\nu)'\boldsymbol{\epsilon}_t = D(\nu, l) \sum_{i=1}^{L} \frac{w_i}{2\lambda_i - \nu} \mathbf{v}_i'\boldsymbol{\epsilon}_t,$$

where $\mathbf{v}_i'\boldsymbol{\epsilon}_t$ is the projection of the data on the i-th Fourier vector $\mathbf{v}_i$. The weights assigned to these projections by $\mathbf{b}(\nu)$ are $\mathbf{w} \odot \mathbf{\Gamma}_{AR(2)}(\nu)$ where $\odot$ designates the Hadamard product: this expression corresponds to the convolution of SSA-AR(2) and $\boldsymbol{\gamma}_\delta$ in the frequency domain. We then refer to $|\mathbf{w}|$ and $\left|\mathbf{w} \odot \mathbf{\Gamma}_{AR(2)}(\nu)\right| = |\mathbf{w}| \odot \left|\mathbf{\Gamma}_{AR(2)}(\nu)\right|$ in terms of (SSA-) amplitude functions of $\boldsymbol{\gamma}_\delta$ and $\mathbf{b}(\nu)$, respectively. Moreover

$$(\mathbf{V}'\mathbf{b}(\nu))'\boldsymbol{\epsilon}_t = \mathbf{b}'\mathbf{V}\boldsymbol{\epsilon}_t = D(\nu, l) \sum_{i=1}^{L} \frac{w_i}{2\lambda_i - \nu} \mathbf{e}_i'\boldsymbol{\epsilon}_t = D(\nu, l) \sum_{i=1}^{L} \frac{w_i}{2\lambda_i - \nu} \epsilon_{t+1-i}$$

where $\mathbf{e}_i$ is the i-th unit vector. The latter expression can be interpreted as a discrete Fourier transform (SSA-DFT) and its square as an SSA periodogram of the predictor. Also

$$\mathbf{b}'(\nu)\mathbf{b}(\nu) = E\left[\mathbf{b}(\nu)'\boldsymbol{\epsilon}_t\boldsymbol{\epsilon}_t'\mathbf{b}(\nu)\right] = E\left[\mathbf{b}(\nu)'\mathbf{V}\boldsymbol{\epsilon}_t\boldsymbol{\epsilon}_t'\mathbf{V}'\mathbf{b}(\nu)\right] = D(\nu, l)^2 \sum_{i=1}^{L} \left(\frac{w_i}{2\lambda_i - \nu}\right)^2$$

is Parseval's identity and $D(\nu, l)^2 \left(\frac{w_i}{2\lambda_i - \nu}\right)^2$ measures the contribution of $\mathbf{v}_i$ to the variance of the predictor. For $\nu \leq -2$, SSA-AR(2) is a highpass with a peak of its transfer (or amplitude) function at frequency π; if $\nu \to -\infty$ then $D(\nu, l)\mathbf{\Gamma}_{AR(2)}(\nu)$ becomes asymptotically an allpass and $\mathbf{b}(\nu) \to \sqrt{l}\boldsymbol{\gamma}_\delta/\sqrt{\boldsymbol{\gamma}_\delta'\boldsymbol{\gamma}_\delta}$, i.e., the SSA predictor converges to the scaled MSE predictor of variance l (degenerate case excluded by Theorem (1)). The highpass favors noise leakage as requested when $ht_1 < ht_{MSE}$ in the holding time constraint. For $\nu \geq 2$, SSA-AR(2) is a lowpass with a peak of its transfer or amplitude function at frequency zero: the filter damps high-frequency noise as requested when $ht_1 > ht_{MSE}$ in the holding time constraint. For $-2 < \nu < 2$, SSA-AR(2) is a bandpass with a peak of its transfer or amplitude function at frequencies $\omega = \pm \arccos(\nu/2)$.

For illustration, we apply the SSA criterion to the quarterly HP filter with parameter $\lambda = 1600$, see Hodrick and Prescott (1997), with two-sided (bi-infinite symmetric) target γ_k displayed in Figure (1). The filter can be interpreted as an optimal MSE-signal extraction filter for the trend in the smooth trend model, see Harvey (1989). We aim at approximating the HP target $z_{t+\delta}$ for $\delta = 0$ by a nowcast y_t based on a one-sided filter b_k, $k = 0, ..., 100$, of length $L = 101$. The MSE nowcast $\boldsymbol{\gamma}_0$ corresponds to the right tail of the two-sided filter and has lag-one ACF $\rho_{MSE} = 0.926$. We compute two SSA nowcasts, imposing lag-one ACFs of $0.97 > \rho_{MSE}$ (smoothing) and $0.8 < \rho_{MSE}$ (un-smoothing) with resulting $\nu_1 = 2.44 > 2$ and $\nu_2 = -2.42 < -2$, see Fig.(1). Optimal smoothing and un-smoothing are obtained by lowpass ($\nu_1 > 2$) and highpass ($\nu_2 < -2$) AR(2)-filters, respectively, and the SSA-amplitude functions $\left|D(\nu_i, l)\mathbf{\Gamma}_{AR(2)}(\nu_i) \odot \mathbf{w}\right|$, $i = 1, 2$, of the corresponding SSA designs are below or above the amplitude $|\mathbf{w}|$ of the MSE benchmark towards higher frequencies, assuming an artificial alignment of all amplitude functions at frequency zero for better visual inspection.

10

Figure 1: HP(1600) and three nowcasts: MSE, SSA(0.97,0) and SSA(0.8,0). Filter coefficients (top graphs) and SSA-amplitude functions (bottom graphs). The first few lags are highlighted in the top rightmost plot. Amplitude of SSA-AR(2) (bottom left), of nowcasts (bottom center) and high frequencies (bottom right). All SSA-amplitude functions are artificially aligned at frequency zero.

The proposed frequency domain analysis suggests that a (unit-root) SSA-AR(2) based on $|\nu| \leq 2$, cannot be reconciled with the optimal tracking of the target at least for large L. Indeed, while ν is always such that $\mathbf{\Gamma}_{AR(2)}(\nu)$ is well defined under the regularity assumptions of Theorem (1), i.e. $\nu \in \mathbb{R} \setminus \{2\lambda_i | i = 1, ..., L\}$, the corresponding SSA-AR(2) transfer function would be subject to an asymptotic singularity at its peak-frequencies $\omega = \pm \arccos(\nu/2)$, as $L \to \infty$, because λ_i are increasingly densely packed in $[-\pi, \pi]$. By assumption (spectral completeness) the spectral weights w_i of $\boldsymbol{\gamma}_\delta$ are non-vanishing, which is invariably the case for classic forecast or signal extraction filters, and therefore the convolution of target and asymptotically unbounded SSA-AR(2) would conflict with an optimal approximation of the former by the latter; moreover, the convolution of SSA-AR(2) with $\boldsymbol{\gamma}_0$ would lead to an asymptotically non-stationary nowcast y_t, strongly periodic, if $-2 \leq \nu < 2$, or strongly trending, if $\nu = 2$, in disagreement with the stationary target specification. In summary, in typical applications, SSA-AR(2) is a lowpass: $\nu > 2$ for enhanced smoothness and the conditions imposed by Corollaries (3), (4) and (6) are not limitations. To conclude we briefly compare classic frequency domain and SSA-amplitude functions in Fig. (2).

11

Figure 2: Comparison of SSA-amplitude (left) and classic amplitude functions (right).

The differences are reliant on the choice of the orthonormal basis for the frequency domain decomposition: $(\exp(-ik\omega))_{k=0,\dots,L-1}$ for the classic approach vs. $(\sin(kj\pi/(L+1)))_{k=1,\dots,L}$ for SSA, noting that the latter basis ensures compliance with the boundary constraints $b_{-1}(\nu) = b_L(\nu) = 0$ since $\sin(kj\pi/(L+1)) = 0$ for $k \in \{0, L+1\}$. The choice of the basis mainly affects the graphical interface for understanding, explaining or interpreting the solution to Criterion (1). In particular, the convolution result $\mathbf{w} \odot \boldsymbol{\Gamma}_{AR(2)}(\nu)$ that helps explain the action of the filter does not hold for the classic basis $(\exp(-ik\omega))_{k=0,\dots,L-1}$.

4.2 MSE, Zero Crossings and Sign Accuracy

Assume ϵ_t to be Gaussian noise and let $\mathrm{SA}(y_t) := \mathrm{P}\Big(\mathrm{sign}(z_{t+\delta}) = \mathrm{sign}(y_t) \Big)$ denote the probability of same sign of target and predictor, where the acronym SA refers to Sign Accuracy. Gaussianity then implies

$$SA(y_t) = 2E\left[I_{\{z_{t+\delta}\geq 0\}}I_{\{y_t\geq 0\}}\right] = 0.5 + \frac{\arcsin(\rho(y,z,\delta))}{\pi}$$

so that maximization of the target correlation $\rho(y,z,\delta)$ or of SA are equivalent optimization principles. The link to SA motivated the choice of the objective function of Criterion (2) in the first place, see Wildi (2024). Proceeding further, we introduce the so-called *holding time* defined by $ht(y|\mathbf{b}, i) := E[t_i - t_{i-1}]$, where t_i, $i \geq 1$ are *consecutive* zero-crossings of y_t, i.e., $t_{i-1} < t_i$, $t_1 \geq L$, $\mathrm{sign}(y_{t_{i-1}}y_{t_i}) < 0$ for all i and $\mathrm{sign}(y_{t-1}y_t) > 0$ if $t_{i-1} < t < t_i$. Under the above stationarity assumptions, $ht(y|\mathbf{b}, i) = ht(y|\mathbf{b})$ measures the expected duration between consecutive zero-crossings of y_t, see Kedem (1986).

Proposition 2. *Let y_t be a zero-mean stationary Gaussian process. Then the holding time $ht(y|\mathbf{b})$ is*

$$ht(y|\mathbf{b}) = \frac{\pi}{\arccos(\rho(y,y,1))}. \tag{24}$$

We refer to Kedem (1986) for proof. The bijective link between the holding time and the lag-one autocorrelation in Equation (24) suggests that Criterion (1) can be interpreted as a maximization of SA under a fixed expected rate of zero crossings of the predictor. Interpreted in its dual form, the predictor generates the fewest crossings in the long term for a given tracking accuracy, see Corollary (6). Table (1) compares target correlations, sign accuracy, lag-one ACF and holding

	HP(1600)	MSE	SSA(0.97,0)	SSA(0.8,0)
Target correlation	1.000	0.733	0.717	0.716
SA	1.000	0.762	0.754	0.754
Lag one ACF	0.996	0.926	0.970	0.800
Holding time	34.316	8.138	12.793	4.882

Table 1: Target correlation, sign accuracy, lag-one ACF and holding time of SSA designs applied to HP

times of the filters in the previous section. A comparison of the holding times of the target and MSE predictor in the first two columns suggests that the latter is subject to substantial leakage. Indeed, unwanted 'noisy' crossings of the predictor are often clustered in the vicinity of target crossings, when both filters hover over the zero line. We then argue that an explicit control of noisy crossings due to an unduly small holding time of the (classic MSE) predictor, is a relevant objective, see Wildi (2024) for an application to real-time business cycle analysis. Moreover, Criterion (1) ensures an optimal tracking of the target by SSA: this property warrants that the interpretation or the economic content supported by z_t, such as, e.g., a business cycle indicator, can be transferred to SSA. Finally, SSA effectively minimizes, if $\nu > 2$, or maximizes, if $\nu < -2$, the rate of zero-crossings in the class of all predictors with the same target correlation (dual interpretation) and therefore Criterion (1) addresses the problem of noisy false alarms in some way optimally. Since zero-crossings, sign accuracy and correlations are indifferent to the scaling of the filter, we can select $s_{MSE} := \mathbf{b}'\boldsymbol{\gamma}_\delta/\mathbf{b}'\mathbf{b}$ such that MSE performances of $s_{MSE}\mathbf{b}$ are optimized conditional on the imposed holding time constraint. In this context, we could look at the alternative MSE criterion

$$\left.\begin{array}{c} \min_{\mathbf{b}}(\boldsymbol{\gamma}_\delta - \mathbf{b})'(\boldsymbol{\gamma}_\delta - \mathbf{b}) \\ \mathbf{b}'\mathbf{M}\mathbf{b} = \mathbf{b}'\mathbf{b}\rho_1 \end{array}\right\}, \tag{25}$$

where the objective function $(\mathbf{b} - \boldsymbol{\gamma}_\delta)'(\mathbf{b} - \boldsymbol{\gamma}_\delta)$ is the MSE and the length constraint is dropped. The corresponding Lagrangian heads to a system of equations for $\mathbf{b}$

$$\begin{array}{rcl} 2(\boldsymbol{\gamma}_\delta - \mathbf{b}) & = & 2\tilde{\lambda}(\mathbf{M} - \rho_1\mathbf{I})\mathbf{b} \\ \boldsymbol{\Psi}^{-1}\mathbf{b} & = & F\boldsymbol{\gamma}_\delta, \end{array}$$

where $\boldsymbol{\Psi} = (2\mathbf{M} - \psi\mathbf{I})$ with $\psi = 2(\rho_1 - 1/\tilde{\lambda})$ and $F = 2/\tilde{\lambda}$. In summary, SSA reconciles MSE, sign accuracy, and smoothing requirements in a flexible and interpretable way. To conclude, we note that the target and predictor can be nearly Gaussian, due to aggregation by the filter (central limit theorem), even if ϵ_t isn't, so that the above transformations, linking correlations, ht and SA, might still be practically relevant despite the violation of the Gaussian assumption: an example is proposed in the appendix and Wildi (2024) shows the resilience of the holding time Equation (24) for an application to the S&P-500 Index, whose log-returns conflict overtly with the Gaussian assumption (extensions to heteroscedastic processes are discussed, too).

5 Forecasting, Signal Extraction and a Prediction Trilemma

5.1 Forecasting

For illustration of the relevant facets of the SSA predictor, we are interested in deriving a one-step-ahead forecast for the MA(2)-process $z_t = \epsilon_t + \epsilon_{t-1} + \epsilon_{t-2}$, where $\gamma_k = 1, k = 0, 1, 2$, $\delta = 1$ and where ϵ_t are assumed to be known, mainly for simplicity of exposition. For this purpose, we compute three different SSA forecast filters $y_{ti}, i = 1, 2, 3$ for z_t: the first two are of identical length $L = 20$ with dissimilar holding times $ht = 3.74$ and 10; the third filter deviates from the second one by selecting $L = 50$; the holding time of the first filter matches the lag-one autocorrelation of z_t and is obtained by inserting $\rho(z, z, 1) = 2/3$ into Equation (24); the second holding time

$ht = 10$ is sufficiently different in size to reveal some of the salient features of the approach. For our comparison we also include the MSE forecast $\hat{z}_{t+1}^{MSE} = \epsilon_t + \epsilon_{t-1}$ as well as a 'lag-by-one' or no-change forecast $\hat{z}_{t+1}^{lag\ 1} = z_t$, see Fig. (3) (an arbitrary scaling scheme is applied to SSA filters).
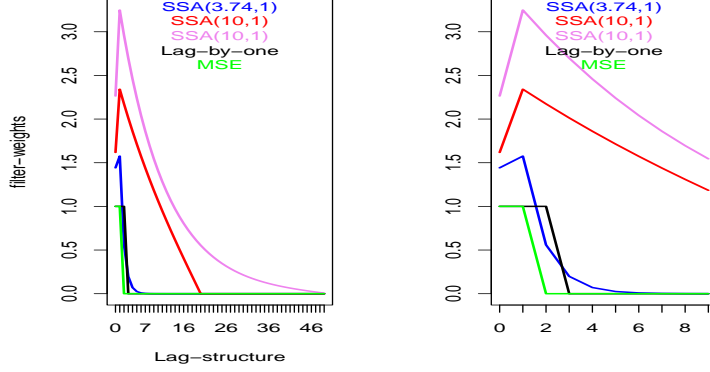

Figure 3: Coefficients of MSE-, SSA- and lag-by-one forecast filters with arbitrarily scaled SSA designs. All lags (left panel) and first ten lags (right panel).

Except for the MSE (green) all other filters rely on past ϵ_{t-k} for $k > q = 2$ which are required for compliance with the holding time constraint (stronger smoothing). For a fixed filter length L, a larger holding time ht asks for a slower zero-decay of filter coefficients (blue vs. red lines) and for fixed holding time ht, a larger L leads to a faster zero-decay but a longer tail of the filter (red vs. violet lines). The distinguishing tips of the SSA filters at lag one in this example are indicative of one of the implicit boundary constraint $b_{-1} = 0$, see Theorem (1). Note that the 'lag-by-one' forecast (black) has the same holding time as the first SSA filter (blue) so that the latter should outperform the former with respect to sign accuracy or, equivalently, in terms of target correlation with the shifted target, as confirmed in Table (2). MSE outperforms all other

	SSA(3.74,1)	SSA(10,1)	SSA(10,1)-long	Lag-by-one	MSE
Target correlation	0.786	0.386	0.388	0.667	0.816
Holding time	3.735	10.000	10.000	3.735	3.000
Sign accuracy	0.788	0.626	0.627	0.732	0.804

Table 2: Performances of MSE and lag-by-one benchmarks vs. SSA. The two columns referring to SSA(10,1) correspond to filter lengths 20 (first) and 50 (second).

forecasts in terms of correlation and sign accuracy but it loses with respect to smoothness or holding time; SSA(3.74,0) outperforms the lag-by-one benchmark; both SSA(10,0) loose in terms of sign accuracy but win with respect to smoothness and while the profiles of longer and shorter filters differ in Figure (3), their respective performances are virtually indistinguishable in Table (2), suggesting that the selection of L is to some extent uncritical, assuming it is at least twice the holding time $L \geq 2ht_1$. The table also illustrates the tradeoff between target correlation (or sign accuracy) and holding time, which is formalized by Equation (6). Table (3) allows for a more detailed analysis based on a finer grid of holding time values. In a business cycle application, MSE performances or, equivalently, the target correlation (first row in the table), are related to assessing the level of the cycle, i.e., its precise value above or below the zero-line, whereas the holding time (second row) emphasizes performances at the zero-line, specifically, with the intent to address the number of random crossings due to noise-leakage of one-sided filters. The SSA framework allows to accord the design of the predictor with the particular purpose of the analysis, by a suitable

	ht=4	ht=4.5	ht=5	ht=5.5	ht=6	ht=7	ht=8	ht=9	ht=10
Target correlation	0.77	0.72	0.68	0.64	0.60	0.53	0.47	0.43	0.39
Emp. ht	4.00	4.50	5.00	5.50	6.00	7.00	8.00	9.00	10.00
Sign accuracy	0.78	0.76	0.74	0.72	0.70	0.68	0.66	0.64	0.63

Table 3: Tradeoff: effect of the holding time on target correlation (first row) and sign accuracy (last row) for fixed forecast horizon.

balance of the observed tradeoff. Different filters could be used, in isolation or combination, for measuring the level with higher accuracy, but reduced smoothness, or for assessing sign changes in the growth rate more reliably, see Wildi (2024). In the latter case, given a specified loss in target correlation, the dual reformulation of the SSA criterion in Corollary (6) asserts that the resulting filter effectively minimizes the rate of zero-crossings or alarms. Formally, a decision for one or several interesting designs could be based on re-computing the above 'tradeoff table' for the particular prediction problem at hand based on the provided SSA package.

In a final step, we allow the previously fixed forecast horizon $\delta = 1$ to vary, see Fig.(4) for illustration.
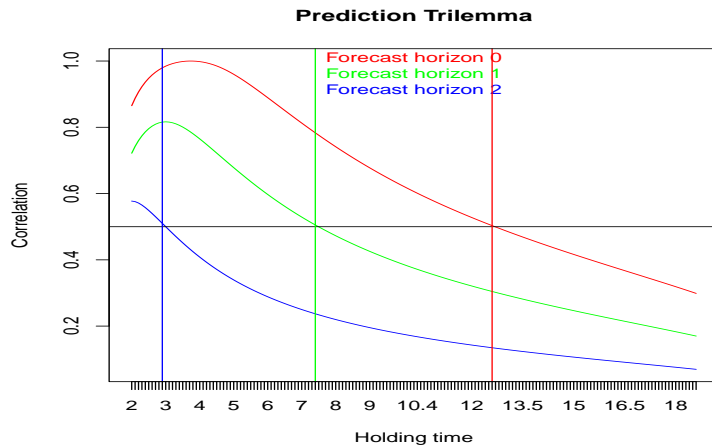

Figure 4: Target correlations of the SSA predictor as a function of the forecast horizon and the holding time.

For each $\delta = 0, 1, 2$, the figure displays the target correlation for given holding times on the abscissa. The peak of the correlation for a given δ appears at a particular holding time value which corresponds to the classic MSE predictor for that forecast horizon: for $\delta = 0$, $y_{t,MSE} = z_t$ and the peak target correlation, obtained at the holding time 3.74 of z_t, is one. To the right of the peak, corresponding to values $\nu > 2$ in Theorem (1), SSA generates fewer crossings (stronger smoothing than MSE) and to its left more ($\nu < -2$); on both sides, SSA maximizes the target correlation, subject to the imposed holding time constraint ht_1 on the abscissa; in its equivalent dual form, SSA maximizes the holding time for given target correlation on the right of the peak ($\nu > 2$), see Corollary (6); finally, the correlation curve for $\delta = 1$ replicates entries in Table (3). For a fixed target correlation, a larger ht_1 (increased smoothness) is functionally related to a smaller δ (reduced timeliness). Specifically, consider the three pairings (ht_{1i}, δ_i), $i = 1, 2, 3$, with values $(2.9, 2)$, $(7.4, 1)$ and $(12.6, 0)$ marked by vertical lines in the figure: the corresponding SSA(ht_{1i}, δ_i)-predictors y_{ti} have a fixed correlation $\rho(y_i, z, \delta_i) = 0.5$ with the target $z_{t+\delta_i}$, marked by the horizontal black line which intersects the curves at the corresponding holding times ht_{1i}, $i = 1, 2, 3$. Fig.(4) generalizes the dilemma in Table (3) to a prediction trilemma, by allowing

15

timeliness, embodied by δ, to become a separate structural element, or hyperparameter, of the estimation problem, together with ht_1. For a particular target $z_{t+\delta_0}$, the pair (ht_1, δ) spans a two-dimensional space of predictors $\text{SSA}(ht_1, \delta)$ and classic MSE performances can be replicated by selecting $\delta = \delta_0$ and $ht_1 = ht_{MSE}$, the holding time of the MSE predictor. However, alternative priorities in terms of timeliness or smoothness can be triggered by screening the two-dimensional predictor space and our SSA package can be used to assess an optimal balance of the constituents of the trilemma for general prediction problems.

5.2 Real-Time Signal Extraction: Addressing Timeliness and Smoothness

We here rely on the HP(1600) target in Section (4.1) and compare performances of three SSA designs when nowcasting the acausal filter: SSA(0.926,0), SSA(0.97, 0) and SSA(0.97, 12). The first design, based on hyperparameters ($\rho_1 = \rho_{MSE}, \delta = 0$) imposes the lag-one ACF of the MSE nowcast and thus replicates the latter; the second design, based on ($\rho_1 = 0.97, \delta = 0$) emphasizes smoothness by imposing a larger lag-one ACF; finally, the third SSA based on ($\rho_1 = 0.97, \delta = 12$) highlights smoothness as well as timeliness (relative lead). As discussed in the previous section, we interpret all three designs as nowcasts of the two-sided HP(1600) emphasizing different priorities, i.e., our effective forecast horizon is $\delta_0 = 0$ and all target correlations are evaluated accordingly. Table (4) summarizes and compares expected and empirical performances, whereby the latter are based on a long sample of (Gaussian) white noise, and Fig.(5) compares a subsample of the

	MSE	SSA(0.97,0)	SSA(0.97,12)
ht	8.138	12.793	12.793
Empirical ht	8.151	12.716	12.793
Target correlation	0.733	0.717	0.512
Emp. correlation	0.732	0.716	0.510

Table 4: Holding times and target correlations of three SSA nowcasts based on different hyperparameter specifications: expected vs. empirical numbers, based on a sample of Gaussian noise of length 100000. All target correlations are computed at $\delta_0 = 0$ (nowcast).

corresponding filter outputs. Our results confirm the prediction trilemma enounced in the previous section: the first SSA (MSE-) nowcast outperforms in terms of target correlation; the other two SSA designs emphasize smoothness equally and together outperform the MSE benchmark; the third nowcast outperforms the other two with respect to timeliness or relative advancement (red line in the figure) but it ranks last according to the target correlation. Interestingly, the timing of its zero-crossings often accords with the acausal target, in contrast to the other two nowcasts which are systematically delayed. In summary, our results confirm that the hyperparameter pairing (δ, ht) of SSA can accommodate various practically relevant research priorities in terms of smoothness, timeliness and target correlation or MSE. Applications of the above concepts to macroeconomic data, including US GDP, industrial production and non-farm payroll are implemented and can be analyzed in our SSA package.
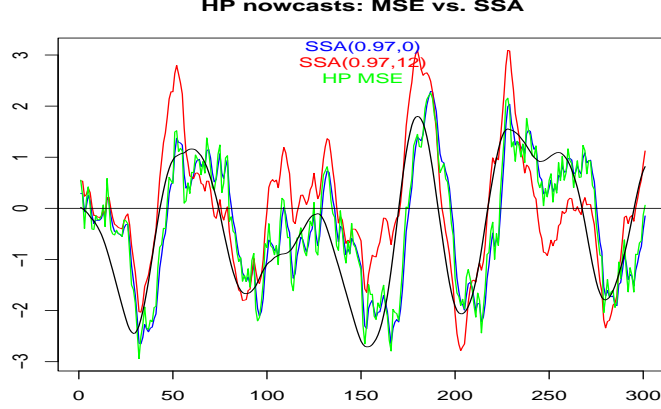
HP nowcasts: MSE vs. SSA

Figure 5: Acausal HP(1600) target (black) and nowcasts: MSE (green), SSA(0.97,0) (blue) and SSA(0.97,12) (red). Both SSA cross the zero line less frequently than MSE and the last SSA (red) is systematically left shifted with a mean lead time or advancement of roughly 1.5 time units when compared to the benchmark. Its zero crossings track the main up- and downturns of the acausal target in a more timely fashion than the other two nowcasts which are prone to a systematic retardation.

6 Autocorrelation

6.1 Stationary Processes

Consider the generalized target $\tilde{z}_t = \sum_{|k|<\infty} \gamma_k x_{t-k}$ where we assume $x_t = \sum_{i=0}^{\infty} \xi_i \epsilon_{t-i}$, with $\xi_0 = 1$, to be an invertible stationary process: the sequence $\boldsymbol{\xi}_{\infty} := (\xi_0, \xi_1, ...)'$ is square summable and corresponds to the weights of the (purely non-deterministic) Wold-decomposition of x_t, see Brockwell and Davis (1993). Let $\boldsymbol{\Xi}$ denote the $L \cdot L$ matrix with i-th row $\boldsymbol{\Xi}_{i \cdot} := (\xi_{i-1}, \xi_{i-2}, ..., \xi_0, \mathbf{0}_{L-i})$, $i = 1, ..., L$, where $\mathbf{0}_{L-i}$ is a zero vector of length $L - i$. Define $\mathbf{x}_t := (x_t, ..., x_{t-(L-1)})'$, $\boldsymbol{\epsilon}_t := (\epsilon_t, ..., \epsilon_{t-(L-1)})'$, $\mathbf{b}_\epsilon := \boldsymbol{\Xi} \mathbf{b}_x$. Then

$$y_t = \mathbf{b}'_x \mathbf{x}_t \approx (\boldsymbol{\Xi} \mathbf{b}_x)' \boldsymbol{\epsilon}_t = \mathbf{b}'_\epsilon \boldsymbol{\epsilon}_t, \tag{26}$$

where the approximation by the finite MA inversion of x_t holds if filter coefficients decay to zero sufficiently rapidly (exact results are proposed in the appendix). The MSE predictor of $z_{t+\delta}$ is derived in McElroy and Wildi (2020)

$$\hat{\gamma}_{x\delta}(B) = \sum_{k \geq 0} \gamma_{k+\delta} B^k + \sum_{k < 0} \gamma_{k+\delta} [\boldsymbol{\xi}(B)]_{|k|}^{\infty} B^k \boldsymbol{\xi}^{-1}(B), \tag{27}$$

where B is the backshift operator, $\boldsymbol{\xi}(B) = \sum_{k \geq 0} \xi_k B^k$, $\boldsymbol{\xi}^{-1}(B)$ denotes the AR-inversion and the notation $[\cdot]_{|k|}^{\infty}$ means omission of the first $|k| - 1$ lags. Intuitively, $\boldsymbol{\xi}^{-1}(B)$ transforms x_t into ϵ_t and $\gamma_{k+\delta} [\boldsymbol{\xi}(B)]_{|k|}^{\infty} B^k$ replicates the weights assigned by the target to present and past ϵ_{t-k}, $k = 0, 1, ...$. Therefore, the prediction error consists of future innovations ϵ_{t+j}, $j > 0$, and is orthogonal to the available data (MSE principle). Let $\hat{\gamma}_{x\delta}$ denote the first L coefficients of the MSE predictor and set $\boldsymbol{\gamma}_{\Xi\delta} := \boldsymbol{\Xi} \hat{\gamma}_{x\delta}$ so that $y_{MSE,t} \approx \hat{\boldsymbol{\gamma}}'_{x\delta} \mathbf{x}_t \approx \boldsymbol{\gamma}'_{\Xi\delta} \boldsymbol{\epsilon}_t$. We are then in a position to generalize Criterion (1)

$$\left. \begin{array}{c} \max_{\mathbf{b}_\epsilon} \mathbf{b}'_\epsilon \boldsymbol{\gamma}_{\Xi\delta} \\ \mathbf{b}'_\epsilon \mathbf{M} \mathbf{b}_\epsilon = \rho_1 \\ \mathbf{b}'_\epsilon \mathbf{b}_\epsilon = 1 \end{array} \right\} \tag{28}$$

17

assuming an arbitrary unit length or unit variance $l = 1$. The SSA solution $\mathbf{b}_x = \mathbf{\Xi}^{-1}\mathbf{b}_\epsilon$ is obtained by solving for $\mathbf{b}_\epsilon$ in Corollary (3), inserting $\boldsymbol{\gamma}_{\Xi\delta}$ for $\boldsymbol{\gamma}_\delta$ in Equation (4). We deduce that autocorrelation of x_t can be interpreted and treated as a modification of the target specification in the original white noise model. If y_t is (nearly) Gaussian, then $ht_1 := \pi / \arccos(\rho_1)$ expresses the holding time of the predictor and the dual interpretation in Corollary (6) applies invariably. An exact expression for the SSA predictor is obtained in the appendix but in order to simplify exposition and to maintain straightforward notations, we now assume pertinence of the finite MA approximation of Equation (26). For illustration, Criterion (28) is applied to the HP target in the previous section, relying on three different AR(1) processes $x_t = a_1 x_{t-1} + \epsilon_t$ with $a_1 = -0.6, 0, 0.6$, see Figure (6).
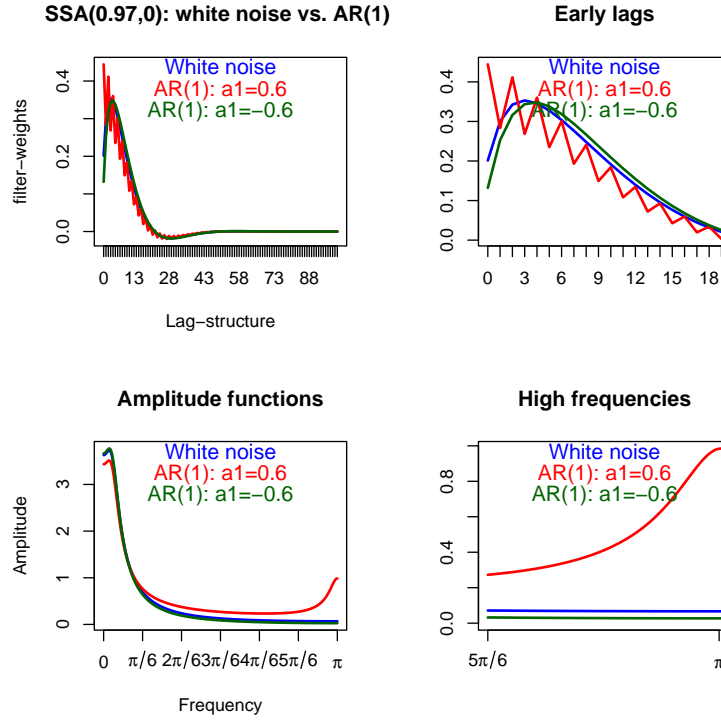

Figure 6: SSA(0.97,0) based on HP(1600)-target. Top left: filters applied to white noise (blue) and AR(1) (red and green); top-right: early lags; bottom-left: classic amplitude functions; bottom-right: classic amplitude towards higher frequencies. All filters are arbitrarily scaled to unit length.

	AR(1)=-0.6	AR(1)=0	AR(1)=0.6
HP MSE	4.344	8.138	14.742
SSA(0.97,0)	12.793	12.793	12.793

Table 5: Holding times of HP (MSE predictor) and SSA as applied to three different AR(1) processes. SSA maintains a fixed holding time across processes.

Table (5) reports holding times of MSE and SSA predictors: while the former depend on the data generating process (DGP), increasing markedly with a_1, the latter remain fixed, irrespective of the DGP. We deduce that the application of a fixed filter to data with unequal dependence structure can lead to qualitatively different components, for example trends or cycles in the case of HP, and SSA can address that ambiguity. For the first two processes in the first two columns

of Table (5), the holding times of HP are smaller than the SSA-specification $ht = 12.79$ and SSA must increase smoothness over the benchmark. In contrast, the holding time $ht = 14.74$ of the benchmark for the third process exceeds the SSA-specification and the latter is asked to generate additional noisy crossings over the benchmark. This atypical demand is reflected by the ripples of the corresponding filter coefficients in Fig.(6). In the frequency domain, the tail behavior of the (classic) amplitude function marks control of the rate of zero-crossings: for $a_1 = -0.6$ the filter damps high-frequency noise most effectively; for $a_1 = 0.6$ increased leakage towards frequency π permits the generation of excess noisy crossings while maintaining optimal tracking of the target by the filter.

6.2 Integrated Processes: Emphasizing Monotonicity

The main modification of the original Criterion (1) for stationary processes concerned the target specification in the objective of Criterion (28), based on the MSE predictor in Equation (27). We now consider an extension to non-stationary integrated processes. In this case, the predictor is generally non-stationary and therefore neither the target correlation nor the rate of zero-crossings are properly defined so that we need to derive a generalization consistent with the previous framework. Let then $\tilde{x}_t$ be such that $\Delta(B)\tilde{x}_t = (1-B)^d \tilde{x}_t =: x_t$ is stationary, invertible and with absolutely summable ACF, such that its spectral density $h_x(\omega)$ exists, and assume $\sum_{k=-\infty}^{\infty} |\gamma_k k^d| < \infty$. In this case, the MSE predictor $y_{t,MSE\infty} := \hat{\gamma}_{\tilde{x}\delta}(B)\tilde{x}_t$ is obtained from

$$\hat{\gamma}_{\tilde{x}\delta}(B) = \sum_{k\geq 0} \gamma_{k+\delta} B^k + \sum_{k<0} \gamma_{k+\delta} \left(\sum_{j=1}^{d} A_{j,d+|k|} B^{d-j} + \sum_{j=1}^{|k|} \psi_{|k|-j} \left[\boldsymbol{\xi}(B) \right]_j^\infty B^{-j} \boldsymbol{\xi}^{-1}(B) \Delta(B) \right), \quad (29)$$

where $(1-B)^d =: 1 - \sum_{j=1}^{d} \delta_j B^j$, $\Psi(B) := 1/\Delta(B) = \sum_{j\geq 0} \psi_k B^k$ and $A_{jt} := \psi_{t-j} - \sum_{k=1}^{d-j} \delta_k \psi_{t-j-k}$, see McElroy and Wildi (2020). Denote the weights of the MSE predictor by $\hat{\boldsymbol{\gamma}}_{\tilde{x}\delta\infty} = (\hat{\gamma}_{\tilde{x}\delta,0}, \hat{\gamma}_{\tilde{x}\delta,1}, ...)'$; then $\sum_{k=0}^{\infty} |\hat{\gamma}_{\tilde{x}\delta,k} k^d| < \infty$ and the so-called cointegration constraints $\sum_{k=-\infty}^{\infty} (\gamma_{k+\delta} - \hat{\gamma}_{\tilde{x}\delta,k}) k^j = 0$, hold for $j = 0, ..., d-1$, where $\hat{\gamma}_{\tilde{x}\delta,k} = 0$ for $k < 0$: these restrictions are necessary to cancel the unit root(s) of $\tilde{x}_t$ by the error filter $e_t := z_{t+\delta} - y_{t,MSE\infty}$ such that e_t is a finite variance stationary process, as a result of MSE optimization. We now assume that similar constraints apply to the SSA predictor: there exists $N > 0$ such that $\sum_{k=0}^{L-1} |b_k k^d| < N$ for all L and $\sum_{k=-\infty}^{\infty} (\gamma_{k+\delta} - b_{\tilde{x}k}) k^j = 0$, for $j = 0, ..., d-1$, see below for a formal implementation. While the general intuition behind the MSE predictor remains the same as for the stationary case, the additional term in $A_{j,d-k}$ accounts for a polynomial $p(t)$ of order $d-1$ of t in the null space of the difference operator $\Delta(B)$, i.e., a solution to the homogeneous difference equation $\Delta(B)p(t) = 0$: the coefficients of this polynomial are determined by a proper initialization of the process (boundary restrictions with permanent effect). We then infer that the MSE predictor can be decomposed into a 'pure' MA inversion and $p(t)$, the latter for matching said boundary constraints. The above cointegration constraints imply that the error filter $\gamma_{k+\delta} - \hat{\gamma}_{\tilde{x}\delta,k}$ cancels a time polynomial of order $d-1$ such that $p(t)$ does not appear in e_t or the MSE anymore.

For further discussion, it is convenient to assume that z_t and $\tilde{x}_t$ are I(1) processes so that $\Delta(B) = 1 - B$, $\psi_k = \begin{cases} 1 & k \geq 0 \\ 0 & \text{otherwise} \end{cases}$, $\sum_{j=1}^{d} A_{j,d+|k|} B^{d-j} = A_{1,1+|k|}$, $A_{1t} := \psi_{t-1}$ and the solution to the homogeneous equation is $p(t) = x_0$, determined by the initialization x_0 at $t = 0$. In this case, the cointegration constraint $\sum_{k=-\infty}^{\infty} (\gamma_{k+\delta} - \hat{\gamma}_{\tilde{x}\delta,k}) = \sum_{k=-\infty}^{\infty} (\gamma_{k+\delta} - b_{\tilde{x}k}) = 0$ cancels $p(t) = x_0$ for both predictors. Let us now introduce some notation: $\boldsymbol{\Sigma}$ is the $L \cdot L$ dimensional summation matrix, with ones along and below the main diagonal, $\boldsymbol{\Delta} := \boldsymbol{\Sigma}^{-1}$ and $\hat{\boldsymbol{\gamma}}_{MSE,L}$ with adjoined $y_{t,MSE}$ denote the finite length MSE predictor, such that the cointegration constraints $\sum_{k=0}^{L-1} \hat{\gamma}_{MSE,k} = \sum_{k=0}^{L-1} b_{\tilde{x}k} = \sum_{k=-\infty}^{\infty} \gamma_{k+\delta}$ apply (we do not need an explicit expression for $\hat{\boldsymbol{\gamma}}_{MSE,L}$ which converges to the infinite length filter in Equation (29) for large L). Then

$$y_{t,MSE} - y_t = (\hat{\boldsymbol{\gamma}}_{MSE,L} - \mathbf{b}_{\tilde{x}})' \tilde{\mathbf{x}}_t = (\hat{\boldsymbol{\gamma}}_{MSE,L} - \mathbf{b}_{\tilde{x}})' \boldsymbol{\Sigma}' \boldsymbol{\Delta}' \tilde{\mathbf{x}}_t = (\hat{\boldsymbol{\gamma}}_{MSE,L} - \mathbf{b}_{\tilde{x}})' \boldsymbol{\Sigma}' \mathbf{x}_t. \quad (30)$$

The last equality holds because the last entry of $(\hat{\boldsymbol{\gamma}}_{\tilde{x}\delta} - \mathbf{b}_{\tilde{x}})'\boldsymbol{\Sigma}'$ vanishes by the cointegration constraint so that the last entry $\tilde{x}_{t-(L-1)}$ of $\boldsymbol{\Delta}'\tilde{\mathbf{x}}_t$ on the left side can be replaced by $x_{t-(L-1)} = \tilde{x}_{t-(L-1)} - \tilde{x}_{t-L}$ on the right side. Now the filter $(\hat{\boldsymbol{\gamma}}_{MSE,L} - \mathbf{b}_{\tilde{x}})'\boldsymbol{\Sigma}'$ is absolutely summable, as $L \to \infty$. To see this let us simplify notation and set $\alpha_k := (\hat{\gamma}_{MSE,k} - b_{\tilde{x}k})$ so that $\boldsymbol{\Sigma}\boldsymbol{\alpha} = (\sum_{j=0}^k \alpha_j)_{k=0,\dots,L-1} = (\sum_{j>k} \alpha_j)_{k=0,\dots,L-1}$ where the last equality holds due to the cointegration constraint which states that $\sum_{k=0}^{L-1} \alpha_k = 0$. The claim of (asymptotic) absolute summability then follows from $\sum_k \left| \sum_{j=0}^k \alpha_j \right| = \sum_k \left| \sum_{j>k} \alpha_j \right| \leq \sum_k |k\alpha_k|$ which is bounded asymptotically, as $L \to \infty$. We then deduce that $y_{t,MSE} - y_t$ has spectral density $|\boldsymbol{\Sigma}(\hat{\boldsymbol{\gamma}}_{MSE,L} - \mathbf{b}_{\tilde{x}})|^2(\omega)h_x(\omega)$ and $(\hat{\boldsymbol{\gamma}}_{MSE,L} - \mathbf{b}_{\tilde{x}})'\boldsymbol{\Sigma}'\mathbf{x}_t \approx (\hat{\boldsymbol{\gamma}}_{MSE,L} - \mathbf{b}_{\tilde{x}})'\boldsymbol{\Sigma}'\boldsymbol{\Xi}'\boldsymbol{\epsilon}_t$, where the error is negligible if the MA-inversion $\xi_k, k \geq 0$ of x_t decays fast enough for given L (for some atypical cases with non-negligible approximation errors, one can resort to the exact solution outlined in the appendix). We then obtain

$$y_{t,MSE} - y_t = (\hat{\boldsymbol{\gamma}}_{MSE,L} - \mathbf{b}_{\tilde{x}})'\boldsymbol{\Sigma}'\mathbf{x}_t \approx (\hat{\boldsymbol{\gamma}}_{MSE,L} - \mathbf{b}_{\tilde{x}})'\boldsymbol{\Sigma}'\boldsymbol{\Xi}'\boldsymbol{\epsilon}_t = \hat{\boldsymbol{\gamma}}'_{MSE,L}\boldsymbol{\Sigma}'\boldsymbol{\Xi}'\boldsymbol{\epsilon}_t - \mathbf{b}'_\epsilon\boldsymbol{\Sigma}'\boldsymbol{\epsilon}_t, \quad (31)$$

where $\mathbf{b}_\epsilon := \boldsymbol{\Xi}\mathbf{b}_{\tilde{x}}$ inherits the cointegration constraint. The processes on the left, i.e., the predictors of $z_{t+\delta}$ are generally non-stationary and cointegrated; the rightmost processes, being based on the finite MA-inversions, are stationary but their variances diverge with increasing L, in contrast to their cross-sectional difference, whose variance remains bounded and whose spectral density is well-defined, asymptotically. We can then interpret $\mathbf{b}'_\epsilon\boldsymbol{\epsilon}_t = (\boldsymbol{\Delta}\boldsymbol{\Sigma}\mathbf{b}_\epsilon)'\boldsymbol{\epsilon}_t = \boldsymbol{\Delta}'(\boldsymbol{\Sigma}\mathbf{b}_\epsilon)'\boldsymbol{\epsilon}_t \approx y_t - y_{t-1}$ as the stationary first difference of the SSA predictor and therefore we can impose a well-defined and interpretable holding time constraint based on the lag-one ACF of $\mathbf{b}'_\epsilon\boldsymbol{\epsilon}_t$. Furthermore, due to stationarity, we can define a proper target correlation. In summary, Equation (31) leads to the following two equivalent expressions for the generalized SSA criterion:

$$\left. \begin{array}{c} \max_{\mathbf{b}_\epsilon} \mathbf{b}'_\epsilon\boldsymbol{\Sigma}'\boldsymbol{\gamma}_{\tilde{\Xi}\delta} \\ \mathbf{b}'_\epsilon\mathbf{M}\mathbf{b}_\epsilon = \rho_1\mathbf{b}'_\epsilon\mathbf{b}_\epsilon \\ \mathbf{b}'_\epsilon\boldsymbol{\Sigma}'\boldsymbol{\Sigma}\mathbf{b}_\epsilon = l \end{array} \right\} \quad \text{or} \quad \left. \begin{array}{c} \min_{\mathbf{b}_\epsilon}(\boldsymbol{\gamma}_{\tilde{\Xi}\delta} - \boldsymbol{\Sigma}\mathbf{b}_\epsilon)'(\boldsymbol{\gamma}_{\tilde{\Xi}\delta} - \boldsymbol{\Sigma}\mathbf{b}_\epsilon) \\ \mathbf{b}'_\epsilon\mathbf{M}\mathbf{b}_\epsilon = \rho_1\mathbf{b}'_\epsilon\mathbf{b}_\epsilon \end{array} \right\}, \quad (32)$$

where $\boldsymbol{\gamma}_{\tilde{\Xi}\delta} := \boldsymbol{\Sigma}\boldsymbol{\Xi}\boldsymbol{\gamma}_{MSE,L}$. The criterion on the left optimizes $\mathbf{b}_\epsilon$ subject to a modified length constraint $\mathbf{b}'_\epsilon\boldsymbol{\Sigma}'\boldsymbol{\Sigma}\mathbf{b}_\epsilon = l$ that warrants proportionality of the objective function and target correlation. The second criterion on the right emphasizes an MSE objective and therefore the length constraint can be skipped. For the left-hand optimization, the derivative of the Lagrangian heads towards a system of equations for $\mathbf{b}_\epsilon$, namely $\boldsymbol{\mathcal{V}}^{-1}\mathbf{b}_\epsilon = D\boldsymbol{\Sigma}'\boldsymbol{\gamma}_{\tilde{\Xi}\delta}$ with $\boldsymbol{\mathcal{V}} := 2\mathbf{M} - 2\rho_1\mathbf{I} + \kappa\boldsymbol{\Sigma}'\boldsymbol{\Sigma}$, $\kappa = 2\tilde{\lambda}_1/\tilde{\lambda}_2$ and $D = 1/\tilde{\lambda}_2$, subject to the cointegration constraint. In this framework, κ can be selected for compliance with the holding time constraint and D is a scaling that ensures compliance with the length constraint (its sign ensures the positiveness of the objective function). Finally, $\mathbf{b}_{\tilde{x}}$ can be obtained from $\boldsymbol{\Xi}^{-1}\mathbf{b}_\epsilon$. Note that the 'pure' MA-inversion on the right of Equation (31) assumes the data to follow a stationary MA-specification such that $\tilde{x}_{t-L} = 0$ for all time points, but the proper SSA predictor $y_t = \mathbf{b}_{\tilde{x}}\mathbf{x}_t$, derived from $\mathbf{b}_\epsilon$, is generally non-stationary. In other words, the finite MA-inversion resumes the relevant information and provides a means for obtaining $\mathbf{b}_{\tilde{x}}$ subject to the imposed cointegration constraint but it is otherwise irrelevant for computing y_t, which is reliant on $p(t)$. Finally, a finite-length truncated version of the predictor in Equation (29) can be inserted for $\hat{\boldsymbol{\gamma}}_{MSE,L}$ in the above criteria. A similar layout applies to the right-hand Criterion (32), for which the derivative of the objective function becomes $-2\boldsymbol{\Sigma}'\boldsymbol{\gamma}_{\tilde{\Xi}\delta} + 2\boldsymbol{\Sigma}'\boldsymbol{\Sigma}\mathbf{b}_\epsilon$ leading to the Lagrangian equations $\left(-\tilde{\lambda}(\mathbf{M} - \rho_1\mathbf{I}) + \boldsymbol{\Sigma}'\boldsymbol{\Sigma}\right)\mathbf{b}_\epsilon = \boldsymbol{\Sigma}'\boldsymbol{\gamma}_{\tilde{\Xi}\delta}$ such that $\tilde{\boldsymbol{\mathcal{V}}}^{-1}\mathbf{b}_\epsilon = F\boldsymbol{\Sigma}'\boldsymbol{\gamma}_{\tilde{\Xi}\delta}$ with $\tilde{\boldsymbol{\mathcal{V}}} := 2\mathbf{M} - 2\rho_1\mathbf{I} - 2/\tilde{\lambda}\boldsymbol{\Sigma}'\boldsymbol{\Sigma}$ and $F := -\frac{2}{\tilde{\lambda}}$. Setting $-2/\tilde{\lambda} = \kappa$ replicates the left-hand side criterion but the scaling F is now fixed to maximize MSE. For a (nearly) Gaussian predictor y_t, $ht_1 := \pi/\arccos(\rho_1)$ expresses the holding time of $y_t - y_{t-1}$: interpreted in its dual form, y_t is 'most monotonic' in the sense that sign changes of $y_t - y_{t-1}$ are fewest possible for a given tracking accuracy.

In the next step, we add structure for tracking the (asymptotically unbounded) level of the non-stationary target by imposing the cointegration constraint to $\mathbf{b}_{\tilde{x}}$. As an introduction, consider

$E[z_t|x_0] = \sum_{|k|<\infty} \gamma_k x_0 = \Gamma(0)x_0$ and $E[y_t|x_0] = \sum_{k=0}^{L-1} b_{xk} x_0 = \hat{\Gamma}_x(0)x_0$, where $\Gamma(\omega), \hat{\Gamma}_x(\omega)$ denote the transfer functions (z-transforms evaluated on the unit circle $z = \exp(i\omega)$) of the sequences $\boldsymbol{\gamma}$ and $\mathbf{b}_{\tilde{x}}$, respectively. We can impose a vanishing bias by requiring $\Gamma(0) = \hat{\Gamma}_x(0)$: in this case $p(t) = x_0$ is canceled in relative terms. Moreover, applying a first-order Taylor approximation to (the transfer function of) the prediction error filter $\Gamma(\omega) - \hat{\Gamma}_x(\omega)$ centered at $\omega = 0$, using $\sum_{|k|<\infty} |\gamma_k k| < \infty$ for computing the derivative, suggests that the error filter cancels the unit root singularity of the pseudo spectral density of x_t such that the prediction error $z_{t+\delta} - y_t$ is stationary, i.e., predictor and target are cointegrated: a corresponding cancellation of the unit root was obtained by Equation (30) in the time domain. Clearly, these properties are desirable in the present context[6] and therefore we now impose the zero-bias or cointegration constraint $\Gamma(0) = \hat{\Gamma}_x(0)$ which can be expressed in vector notation as $\mathbf{b}_{\tilde{x}} = \Gamma(0)\mathbf{e}_1 + \mathbf{B}\tilde{\mathbf{b}}$, where $\mathbf{B}$ is an $L \cdot (L-1)$ dimensional matrix, whose first row, filled with -1, is stacked on the $(L-1) \cdot (L-1)$ identity, and where the unit vector $\mathbf{e}_1 = (1, 0, ..., 0)'$ and $\tilde{\mathbf{b}} = (\tilde{b}_1, ..., \tilde{b}_L)'$ are of length L and $L-1$, respectively. We then obtain

$$\mathbf{b}_\epsilon' \mathbf{M} \mathbf{b}_\epsilon = \mathbf{b}_{\tilde{x}}' \mathbf{\Xi}' \mathbf{M} \mathbf{\Xi} \mathbf{b}_{\tilde{x}} = \Gamma(0)^2 \mathbf{e}_1' \mathbf{\Xi}' \mathbf{M} \mathbf{\Xi} \mathbf{e}_1 + 2\Gamma(0)\mathbf{e}_1' \mathbf{\Xi}' \mathbf{M} \mathbf{\Xi} \mathbf{B} \tilde{\mathbf{b}} + \tilde{\mathbf{b}}' \mathbf{B}' \mathbf{\Xi}' \mathbf{M} \mathbf{\Xi} \mathbf{B} \tilde{\mathbf{b}}$$

A similar expression is obtained for $\mathbf{b}_\epsilon' \mathbf{b}_\epsilon$, replacing $\mathbf{M}$ by $\mathbf{I}$ in the above expression. Then, the holding-time constraint of (either) Criterion (32) becomes

$$\Gamma(0)^2 \mathbf{e}_1' \mathbf{\Xi}' \mathcal{V}_{\rho_1} \mathbf{\Xi} \mathbf{e}_1 + 2\Gamma(0)\mathbf{e}_1' \mathbf{\Xi}' \mathcal{V}_{\rho_1} \mathbf{\Xi} \mathbf{B} \tilde{\mathbf{b}} + \tilde{\mathbf{b}}' \mathbf{B}' \mathbf{\Xi}' \mathcal{V}_{\rho_1} \mathbf{\Xi} \mathbf{B} \tilde{\mathbf{b}} = \mathbf{0},$$

where $\mathcal{V}_{\rho_1} = \mathbf{M} - \rho_1 \mathbf{I}$. Taking derivatives with respect to $\tilde{\mathbf{b}}$ gives $2\Gamma(0)\mathbf{e}_1' \mathbf{\Xi}' \mathcal{V}_{\rho_1} \mathbf{\Xi} \mathbf{B} + 2\mathbf{B}' \mathbf{\Xi}' \mathcal{V}_{\rho_1} \mathbf{\Xi} \mathbf{B} \tilde{\mathbf{b}}$. For the objective function we can rely on the right hand (MSE-) SSA criterion:

$$
\begin{aligned}
(\boldsymbol{\gamma}_{\tilde{\Xi}\delta} - \mathbf{\Sigma}\mathbf{b}_\epsilon)'(\boldsymbol{\gamma}_{\tilde{\Xi}\delta} - \mathbf{\Sigma}\mathbf{b}_\epsilon) &= (\boldsymbol{\gamma}_{\tilde{\Xi}\delta} - \tilde{\mathbf{\Xi}}\mathbf{b}_{\tilde{x}})'(\boldsymbol{\gamma}_{\tilde{\Xi}\delta} - \tilde{\mathbf{\Xi}}\mathbf{b}_{\tilde{x}}) \\
&= \left(\boldsymbol{\gamma}_{\tilde{\Xi}\delta} - \tilde{\mathbf{\Xi}}\left[\Gamma(0)\mathbf{e}_1 + \mathbf{B}\tilde{\mathbf{b}}\right]\right)'\left(\boldsymbol{\gamma}_{\tilde{\Xi}\delta} - \tilde{\mathbf{\Xi}}\left[\Gamma(0)\mathbf{e}_1 + \mathbf{B}\tilde{\mathbf{b}}\right]\right),
\end{aligned}
$$

where $\tilde{\mathbf{\Xi}} := \mathbf{\Sigma}\mathbf{\Xi}$. Its derivative is $2\mathbf{B}'\tilde{\mathbf{\Xi}}'\left(\boldsymbol{\gamma}_{\tilde{\Xi}\delta} - \tilde{\mathbf{\Xi}}\left[\Gamma(0)\mathbf{e}_1 + \mathbf{B}\tilde{\mathbf{b}}\right]\right) = 2\mathbf{B}'\tilde{\mathbf{\Xi}}'\left(\boldsymbol{\gamma}_{\tilde{\Xi}\delta} - \Gamma(0)\tilde{\mathbf{\Xi}}\mathbf{e}_1\right) - 2\mathbf{B}'\tilde{\mathbf{\Xi}}'\tilde{\mathbf{\Xi}}\mathbf{B}\tilde{\mathbf{b}}$. Plugging both derivatives into the Lagrangian and equating to zero heads towards a system of equations for $\tilde{\mathbf{b}}$

$$\tilde{\mathbf{b}} = -\left(\mathbf{B}'\tilde{\mathbf{\Xi}}'\tilde{\mathbf{\Xi}}\mathbf{B} + \lambda\mathbf{B}'\mathbf{\Xi}'\mathcal{V}_{\rho_1}\mathbf{\Xi}\mathbf{B}\right)^{-1}\left\{-\mathbf{B}'\tilde{\mathbf{\Xi}}'\boldsymbol{\gamma}_{\tilde{\Xi}\delta} + \Gamma(0)\mathbf{B}'\tilde{\mathbf{\Xi}}'\tilde{\mathbf{\Xi}}\mathbf{e}_1 + \lambda\Gamma(0)\mathbf{B}'\mathbf{\Xi}'\mathcal{V}_{\rho_1}\mathbf{\Xi}\mathbf{e}_1\right\} \quad (33)$$

The solution to the right hand (MSE) Criterion (32), subject to the cointegration constraint, reparameterized in terms of $\tilde{\mathbf{b}}$, is obtained from Equation (33) whereby $\tilde{\lambda}$ must be selected for compliance with the holding time constraint: $\mathbf{b}_\epsilon' \mathbf{M} \mathbf{b}_\epsilon = \rho_1 \mathbf{b}_\epsilon' \mathbf{b}_\epsilon$ where $\mathbf{b}_\epsilon = \mathbf{\Xi}\left(\Gamma(0)\mathbf{e}_1 + \mathbf{B}\tilde{\mathbf{b}}\right)$. Extensions to higher order integration orders $d > 1$ can be obtained by using the summation operator $\mathbf{\Sigma}^d$ in the above expressions, assuming γ_k to be such that $\sum_{|k|<\infty} |\gamma_k k^d| < \infty$ and by imposing additional (cointegration) constraints of the form $\sum_{k=0}^{L-1} b_{\tilde{x}k} k^j = \sum_{k=-\infty}^{\infty} \gamma_k k^j$, $j = 0, ..., d-1$, canceling the higher order polynomial $p(t)$ of Equation (29) in relative terms and ensuring stationarity of the prediction error[7]. An explicit extension to the practically relevant I(2)-case can be found in the appendix.

6.3 Forecasting Revisited

The forecast problem in Section (5.1) based on the MA(3) $z_t = \epsilon_t + \epsilon_{t-1} + \epsilon_{t-2}$ process can be expressed alternatively by assigning the role of the dependency structure of the target to the MA-inversion of x_t, i.e., $x_t = \epsilon_t + \epsilon_{t-1} + \epsilon_{t-2}$, $\xi_0 = \xi_1 = \xi_3 = 1$, $z_{t+\delta} = x_{t+\delta}$ and $\gamma_k = \begin{cases} 1 & k = 0 \\ 0 & \text{otherwise} \end{cases}$

---

[6] The constraint could be imposed in the stationary case, too, but the benefit of improved level tracking is more explicit for integrated processes with asymptotically unbounded paths. An application to series which are stationary up to episodic level-shifts can be envisioned, too.

[7] One can use a d-th order Taylor approximation of the error filter $\Gamma(\omega) - \hat{\Gamma}_x(\omega)$ centered at $\omega = 0$ to show that the error filter cancels the d-th order singularity of the pseudo-spectral density of x_t.

which is a more natural or common problem formulation. The main distinguishing feature of forecasting is that the target filter $\gamma_{k+\delta}$ is an acausal identity or an anticipative *allpass* filter. In contrast, signal extraction is about the isolation of specific components in terms of acausal lowpass (trend: HP), bandpass (cycle: BK filter), multi-trough (seasonal adjustment) or highpass (HP-gap: identity minus HP-trend). Finally, smoothing is about *causal* targets.

7 Smoothing

7.1 SSA vs. Whittaker-Henderson and Hodrick Prescott

An interesting simple SSA problem is obtained when selecting $\boldsymbol{\gamma} = 1$ the identity and $\delta = -(L-1)/2$ (backcast), assuming L to be an odd number. In this case, Criterion (2) becomes

$$\left. \begin{array}{c} \max_{\mathbf{b}} \rho\Big(y, x, \delta = -(L-1)/2\Big) \\ \rho(y, y, 1) = \rho_1 \end{array} \right\} \tag{34}$$

and its solution y_t aims at tracking $x_{t+\delta}$ while being smoother if $\rho_1 > \rho(x, x, 1)$, the lag-one ACF of the data. Selecting $\delta = -(L-1)/2$ ensures symmetry of the backcast: the coefficients of the causal filter are centered at $x_{t-(L-1)/2}$ and the tails are mirrored at the center point. Let then $\tilde{y}_t := y_{t-\delta}$ denote the so-called SSA smoother, the solution to Criterion (34) shifted forward and centered at x_t. We can contrast our approach with classic Whittaker-Henderson (WH) smoothing, Whittaker (1922) and Henderson (1924), who propose to solve the following optimization problem for $\mathbf{u} := (u_1, ..., u_T)$

$$\min_{\mathbf{u}} \left(\sum_{t=1}^{T} (x_t - u_t)^2 + \lambda \sum_{t=d+1}^{T} (\Delta^d u_t)^2 \right).$$

The HP filter is obtained by selecting $d = 2$, emphasizing squared second-order differences, i.e., the curvature, in the penalty term. In the case of stationary data, increasing λ typically leads to a longer holding time of u_t but Criterion (34) is more apt at controlling this particular characteristic. For illustration, Fig.(7) displays HP and two different SSA smoothers, all based on a fixed length $L = 201$, and Table (6) compares their performances. For an identical holding time, SSA1 (blue

	HP	SSA1	SSA2
Holding times	34.366	34.366	42.830
Target correlations	0.271	0.301	0.271
RMS second-order differences	0.204	0.757	0.547

Table 6: HP vs. two different SSA smoothers. SSA1 replicates the holding time of HP and SSA2 replicates its target correlation. Root mean-square second-order differences in the last row refer to standardized white noise data.

line in the figure) outperforms HP in terms of target correlation. In virtue of Corollary (6), SSA2 (violet line in the figure) outperforms HP according to the holding time for given identical target correlation. However, HP wins with respect to mean-square second-order differences. The observed discrepancies in each one of the reported performance measures seem sufficiently important to ask for an informed decision: minimizing the rate of zero-crossings, by SSA, or minimizing the curvature, by WH.
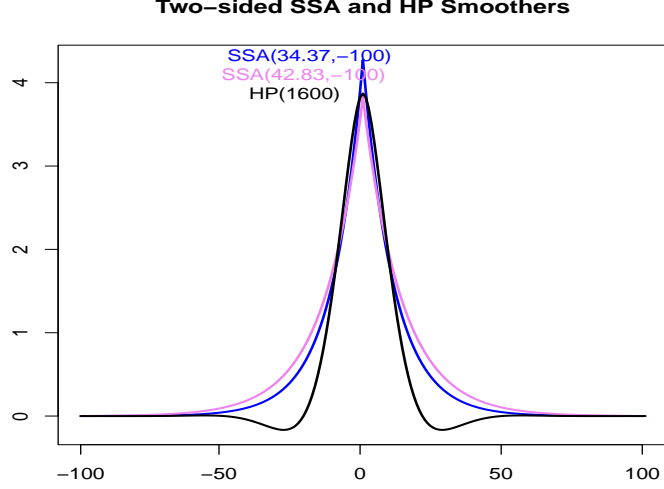
Figure 7: Coefficients of two-sided SSA and HP smoothers of length 401, arbitrarily scaled to unit length: the first SSA design (blue line) replicates the holding time of HP, the second SSA design (violet line) replicates the tracking-ability or target correlation of HP.

To conclude, we broaden the scope of the above comparison. An optimal causal or one-sided SSA 'smoother' can be obtained straightforwardly, by specifying $\delta = 0$, instead of $\delta = -(L-1)/2$, in Criterion (34). Furthermore, the original Criterion (1) or its extensions (28), (32) or (33) address more general estimation or prediction problems than the simple identity-smoothing (34), based on $\gamma = 1$. Finally, SSA can accommodate for the DGP in terms of the MA inversion of x_t. We argue that if a predictor, or a smoother, has to match sign changes of a target while keeping control of the alarming rate, determined by zero-crossings, as well as of MSE performances and timeliness characteristics, then the hyperparameters ρ_1, δ of SSA, as well as the underlying optimization principle, address facets of that problem in a more nuanced way than λ for the WH smoother and, incidentally, for the HP filter.

7.2 SSA Plug On and Benchmark Customization

We here extend the concept of smoothing to arbitrary causal targets, whereby causality is the distinguishing feature when compared to prediction: Wildi (2024) applies SSA to the classic one-sided concurrent HP trend filter; in addition, Hamilton (2018) as well as (one-sided) Baxter and King (1999) filters are implemented in the SSA package. In this context, we can apply Criterion (1) 'as is', inserting x_t for ϵ_t irrespective of the true dependence structure of x_t; alternatively, we can apply its extensions to autocorrelated data in Section (6), benefiting of a model for the DGP. In both cases, SSA is 'plugged' on an existing (causal) benchmark $\hat{\gamma}$ to address smoothness: if the DGP is modeled correctly, then the holding time constraint can be interpreted literally, assuming y_t to be (nearly) Gaussian, see Table (5); otherwise, the holding time constraint is a generic smoothing requirement, much like the curvature penalty of the Whittaker-Henderson approach. The resulting smoother can be interpreted as a customized benchmark tracking the objective as closely as possible subject to smoothness and timeliness 'priorities' entailed by ρ_1, δ: MSE optimality can be invoked if the DGP is modeled correctly, eventually up to an arbitrary scaling constant, and therefore we argue that the SSA-smoother inherits the meaning or interpretation of the causal benchmark in this case.

8 Conclusion

We propose a novel SSA criterion that emphasizes sign accuracy and zero-crossings of the predictor subject to a holding time constraint. The classic MSE approach is equivalent to unconstrained SSA-optimization: in the absence of a holding time constraint and down to an arbitrary scaling nuisance. In its primal form, SSA aims at tracking the target optimally subject to an imposed noise suppression; in its dual form, the predictor generates the least zero-crossings for given track accuracy. Moreover, the SSA predictor is interpretable and appealing due to its actual simplicity and because the underlying criterion merges relevant concepts of prediction in terms of sign accuracy, MSE, and smoothing requirements which can be merged with timeliness, i.e. retardation or advancement, to constitute a prediction trilemma. The application to real-time signal extraction, based on the HP target, illustrates that the timeliness and smoothness of real-time designs can be controlled effectively. Furthermore, interpretability and economic content can be transferred from the target to the SSA predictor, due to optimality of the approximation. Finally, an alternative to classic Whittacker Henderson smoothing can be obtained by inserting the identity for the target in the optimization criterion and the resulting SSA smoother can address zero-crossings and MSE-performances explicitly.

9 Appendix

9.1 Theoretical vs. Empirical Holding Times for t-Distributed Random Variables

Table (7) evaluates the effect of heavy tails on holding times of the SSA nowcasts of Section (3). Heavier tails increase the positive holding time bias because extreme observations can trigger the

	MSE	SSA(0.97,-100)	SSA(0.8,-100)
t-dist.: df=2.1	9.89	14.14	5.98
t-dist.: df=4	8.87	13.34	5.32
t-dist.: df=6	8.55	13.10	5.14
t-dist.: df=8	8.44	13.01	5.04
t-dist.: df=10	8.30	12.89	4.98
t-dist.: df=100	8.16	12.83	4.90
Gaussian	8.14	12.79	4.88

Table 7: The effect of heavy tails on the empirical holding times of HP predictors, based on samples of length one Million: Gaussian vs. t-distributed data.

impulse response, which does not change signs frequently. On the other hand, the central limit effect works against this bias in the sense that stronger smoothing of the non-Gaussian noise by the filter can narrow the gap separating the predictor from Gaussianity: as an example, the filter in the second column seems least affected by distortions of the holding time, in relative terms. In any case, $ht = ht_\mathbf{b} := \pi/\arccos(\rho(y, y, 1)$ is named holding time: if y_t is (nearly) Gaussian, then the mean duration between consecutive zero crossings converges to ht for long samples. An extension to (conditional) heteroscedastic processes is discussed in Wildi (2024) who illustrates that SA and ht are fairly robust against vola-clustering.

9.2 Spherical Length- and Hyperbolic Holding-Time Constraints

Consider the spectral decomposition

$$\mathbf{b} := \sum_{i=1}^{L} \alpha_i \mathbf{v}_i \tag{35}$$

24

where $\sum_{i=1}^{L} \alpha_i^2 = 1$ (unit-sphere constraint, i.e., we assume $l = 1$ in the length constraint). Moreover, $\rho_1 = \mathbf{b}'\mathbf{M}\mathbf{b} = \sum_{i=1}^{L} \alpha_i^2 \lambda_i$ so that $\alpha_{j_0} = \pm\sqrt{\frac{\rho_1}{\lambda_{j_0}} - \sum_{k\neq j_0} \alpha_k^2 \frac{\lambda_k}{\lambda_{j_0}}}$, where j_0 is such that $\lambda_{j_0} \neq 0$. The SSA problem can be solved if the hyperbola, defined by the holding-time constraint, intersects the unit-sphere. Plugging the former into the latter we obtain

$$\alpha_{i_0}^2 = 1 - \sum_{i\neq i_0} \alpha_i^2 = 1 - \left(\frac{\rho_1}{\lambda_{j_0}} - \sum_{k\neq j_0} \alpha_k^2 \frac{\lambda_k}{\lambda_{j_0}}\right) - \sum_{i\neq i_0,j_0} \alpha_i^2$$

assuming $i_0 \neq j_0$. Solving for α_{i_0} then leads to

$$\alpha_{i_0} = \pm\sqrt{\frac{\lambda_{j_0} - \rho_1}{\lambda_{j_0} - \lambda_{i_0}} - \sum_{k\neq i_0, k\neq j_0} \alpha_k^2 \frac{\lambda_{j_0} - \lambda_k}{\lambda_{j_0} - \lambda_{i_0}}} \tag{36}$$

We now examine the case $\rho_1 = -\rho_{max}(L) = \lambda_L$ and set $i_0 = L$:

$$\alpha_L = \pm\sqrt{1 - \sum_{k\neq L, k\neq j_0} \alpha_k^2 \frac{\lambda_{j_0} - \lambda_k}{\lambda_{j_0} - \lambda_L}} \tag{37}$$

For $j_0 = L-1$ we have $\lambda_{L-1} - \lambda_k < 0$ in the nominators of the summands of 37 and $\lambda_{L-1} - \lambda_L > 0$ in the denominators. We then deduce that if $\alpha_k \neq 0$ for some $k < L - 1$, then $|\alpha_L| > 1$ which would contradict the unit-sphere constraint. Therefore, $\alpha_k = 0$ for $k < L - 1$ so that $\alpha_L = \pm 1$, $\alpha_{L-1} = 0$ and $\mathbf{b} := \pm\mathbf{v}_L$ (the contacts of unit-sphere and hyperbola are tangential at the vertices $\pm\mathbf{v}_L$). Since $w_L \neq 0$ (completeness assumption), the SSA solution $\mathbf{b} := \mathrm{sign}(w_L)\mathbf{v}_L$ warrants a positive objective function $\boldsymbol{\gamma}_\delta'\mathbf{b} = \mathrm{sign}(w_L)w_L > 0$, confirming Corollary (1). Next, for $\rho_1 > \lambda_L$ the quotient $\frac{\lambda_{L-1}-\rho_1}{\lambda_{L-1}-\lambda_L}$ in (36) is smaller one which allows for non-vanishing $\alpha_k \neq 0$, $k < L - 1$, in Equation (37). However, in this case the number under the square root should remain positive which is always the case for $\rho_1 \leq \rho_{max}(L) = \lambda_1$ since the term $-\alpha_1^2 \frac{\lambda_{L-1}-\lambda_1}{\lambda_{L-1}-\lambda_L}$ of the sum $-\sum_{k<L-1} \alpha_k^2 \frac{\lambda_{L-1}-\lambda_k}{\lambda_{L-1}-\lambda_L}$ can compensate for a potentially negative value of $\frac{\lambda_{L-1}-\rho_1}{\lambda_{L-1}-\lambda_L}$. In particular, if $\rho_1 = \rho_{max}(L)$, then positiveness of the term under the square root implies $\alpha_1 = 1$ and $\alpha_2, ..., \alpha_{L-2} = 0$, by symmetry, so that $\alpha_L = \alpha_{L-1} = 0$, i.e., $\mathbf{b} = \pm v_1$, confirming again Corollary (1). In between, that is for $\rho_{min}(L) < \rho_1 < \rho_{max}(L)$, the number under the square root is in the open unit interval $]0,1[$ and the intersection of the unit sphere and holding time hyperbola is non-empty and of dimension $L - 2 \geq 1$.

9.3 The Choice of M

The matrix $\mathbf{M}$ is not uniquely determined by the quadratic form $\mathbf{b}'\mathbf{M}\mathbf{b} = \sum_{k=1}^{L-1} b_{k-1} b_k$. Indeed, the family of corresponding matrices $\mathbf{M}(\kappa)$ has zeroes everywhere except above and below the main diagonal, where the corresponding entries are κ and $1 - \kappa$, respectively

$$\mathbf{M}(\kappa) = \begin{pmatrix} 0 & \kappa & 0 & 0 & 0 & ... & 0 & 0 & 0 \\ 1-\kappa & 0 & \kappa & 0 & 0 & ... & 0 & 0 & 0 \\ ... & & & & & & & & \\ 0 & 0 & 0 & 0 & 0 & ... & 1-\kappa & 0 & \kappa \\ 0 & 0 & 0 & 0 & 0 & ... & 0 & 1-\kappa & 0 \end{pmatrix},$$

with $\kappa \in \mathbb{R}$: for $\kappa = 0.5$ the original $\mathbf{M} := \mathbf{M}(0.5)$ is obtained. Evidently, all obtained results straightforwardly extend to $\mathbf{M}(\kappa)$, noting that derivatives of quadratic forms would involve $\mathbf{M}(\kappa) + \mathbf{M}(\kappa)' = 2\mathbf{M}(0.5)$ so that κ is canceled. More generally, the technical elements of the proof of Theorem (1) assume $\mathbf{M}$ to be symmetric with pairwise different eigenvalues and therefore the theorem would apply to constraints of the ACF at higher lags, though this possibility is neither explicitly required nor explored here.

9.4 Illustration of a Case of Incomplete Spectral Support

To illustrate the case of incomplete spectral support addressed by Corollary (2), we propose a simple nowcast example, $\delta = 0$, based on a band-limited target $\gamma_0 = \sum_{i=4}^{10} 0.378\mathbf{v}_i$ of length $L = 10$, where $\mathbf{v}_i$ are the eigenvectors of the $10 \cdot 10$-dimensional $\mathbf{M}$, assuming that the first three weights $w_1 = w_2 = w_3 = 0$ vanish ($n = 4$ in Equation (3)) and that the last seven weights are constant $w_i = 0.378$: this particular weighting scheme implies that $\gamma_0'\gamma_0 = 1$ such that the SSA objective function is also the target correlation. The left panel in Fig. 8 displays the lag-one ACF 17 of $\mathbf{b}(\nu)$ given by 16 as a function of $\nu \in [-2, 2] - \{2\lambda_i, i = 1, ..., L\}$, thus omitting all potential singularities at $\nu = 2\lambda_i$, $i = 1, ..., L$; the right panel displays additionally the lag-one ACF 19 of the extension $\mathbf{b}_{i_0}(\tilde{N}_{i_0})$ in 18, when $\nu = \nu_{i_0} = 2\lambda_{i_0}$ for $i_0 = 1, 2, 3$, where the three additional (vertical black) spectral lines, corresponding to $\mathbf{v}_1, \mathbf{v}_2, \mathbf{v}_3$, show the range of ACF-values as a function of $\tilde{N}_{i_0} \in \mathbb{R}$: lower and upper bounds of each spectral line correspond to $\rho_{i_0}(0) = \rho_{\nu_{i_0}} = \frac{M_{i_0 1}}{M_{i_0 2}}$, when $\tilde{N}_{i_0} = 0$ in 19, and $\rho_{i_0}(\pm\infty) = \lambda_{i_0}$, when $\tilde{N}_{i_0} = \pm\infty$. The green horizontal lines in both graphs correspond to two different arbitrary holding-times $\rho_1 = 0.6$ and $\rho_1 = 0.365$: the intersections of the latter with the ACF, marked by colored vertical lines in each panel, indicate potential solutions to the SSA problem for the thusly specified holding time constraint. The corresponding criterion values are reported at the bottom of the colored vertical lines: the SSA solution is determined by the intersection which leads to the highest criterion value (rightmost in this example).
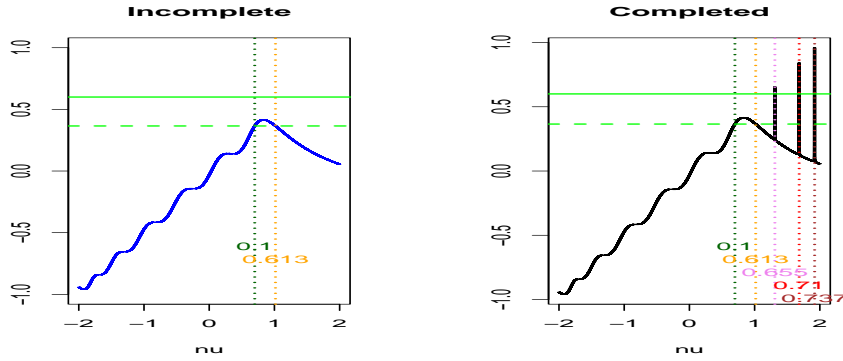

Figure 8: Lag-one autocorrelation as a function of ν. Original (incomplete) solutions (left panel) vs. completed solutions (right panel). Intersections of the ACF with the two green lines are potential solutions to the SSA problem for the corresponding holding times: criterion values are reported for each intersection (bottom right).

The right panel in the figure illustrates that the completion with the extensions $\mathbf{b}_{i_0}(\tilde{N}_{i_0})$ at the singular points $\nu = \nu_{i_0} = 2\lambda_{i_0}$ for $i_0 = 1, 2, 3$ can accommodate for a wider range of holding-time constraints, such that $|\rho_1| < \rho_{max}(L) = \lambda_1 = 0.959$; in contrast, $\mathbf{b}(\nu)$ in the left panel is limited to $-0.959 = \lambda_{10} < \rho_1 < \lambda_4 = 0.415$ so that there does not exist a solution for $\rho_1 = 0.6$ (no intersection with upper green line in left panel). Moreover, for a given holding-time constraint, the additional stationary points corresponding to intersections at the spectral lines of the (completed) ACF might lead to improved performances, as shown in the right panel, where the maximal criterion value

$$\left(\mathbf{b}_{i_0}(\tilde{N}_{i_0})\right)' \gamma_\delta = \left(\mathbf{b}_{10}(0.077)\right)' \gamma_0 = 0.737$$

is attained at the right-most spectral line, for $i_0 = 1$, and where $\tilde{N}_1 = 0.077$ has been obtained from 20, with the correct signs of D and $\tilde{N}_1$ in place.

9.5 Proofs of Corollaries (2) and (4)

Proof of Corollary (2): The first assertion follows directly from the Lagrangian Equation (8). Under the case posited in the second assertion, $\boldsymbol{\nu}_{i_0}$ is not of full rank and $\mathbf{b}_{i_0}(\tilde{N}_{i_0})$ as defined by Equation (18) is a solution to the Lagrangian equation $D\boldsymbol{\gamma}_\delta = \boldsymbol{\nu}_{i_0}\mathbf{b}_{i_0}(\tilde{N}_{i_0})$ for arbitrary $\tilde{N}_{i_0}$. Moreover,

$$\rho_{i_0}(\tilde{N}_{i_0}) := \frac{\mathbf{b}_{i_0}(\tilde{N}_{i_0})'\mathbf{M}\mathbf{b}_{i_0}(\tilde{N}_{i_0})}{\mathbf{b}'_{i_0}(\tilde{N}_{i_0})\mathbf{b}_{i_0}(\tilde{N}_{i_0})} = \frac{\sum_{i \neq i_0} \lambda_i w_i^2 \frac{1}{(2\lambda_i - \nu)^2} + \tilde{N}_{i_0}^2 \lambda_{i_0}}{\sum_{i \neq i_0} w_i^2 \frac{1}{(2\lambda_i - \nu)^2} + \tilde{N}_{i_0}^2} = \frac{M_{i_0 1} + \tilde{N}_{i_0}^2 \lambda_{i_0}}{M_{i_0 2} + \tilde{N}_{i_0}^2}.$$

Solving for the holding-time constraint $\rho_{i_0}(\tilde{N}_{i_0}) = \rho_1$ then leads to $N_{i_0} := \tilde{N}_{i_0}^2 = \frac{\rho_1 M_{i_0 2} - M_{i_0 1}}{\lambda_{i_0} - \rho_1}$. We infer that N_{i_0} is positive if $0 < \rho(\nu_{i_0}) = \frac{M_{i_0 1}}{M_{i_0 2}} < \rho_1 < \lambda_{i_0}$ or $0 > \rho(\nu_{i_0}) = \frac{M_{i_0 1}}{M_{i_0 2}} > \rho_1 > \lambda_{i_0}$, so that $\tilde{N}_{i_0} = \pm\sqrt{N_{i_0}} \in \mathbb{R}$, as claimed. Finally, the correct sign combination of the pair $D, \tilde{N}_{i_0}$ is determined by the maximal criterion value. For a proof of the third and last assertion, we first assume that $\boldsymbol{\gamma}_\delta$ is not band-limited so that $w_1 \neq 0$ and $w_L \neq 0$. Then, $\lim_{\nu \to 2\lambda_1} \rho(\nu) = \lambda_1 = \rho_{max}(L)$ and $\lim_{\nu \to 2\lambda_L} \rho(\nu) = \lambda_L = -\rho_{max}(L)$, see the proof of Theorem (1). By continuity of $\rho(\nu)$ and by the intermediate-value theorem, any ρ_1 such that $|\rho_1| \leq \rho_{max}(L)$ is admissible for the holding-time constraint. Otherwise, if $w_1 = 0$ then $\mathbf{b}_1(\tilde{N}_1)$, where $i_0 = 1$ in Equation (18), can 'fill the gap' and approach the upper boundary $\rho_{max}(L)$ arbitrarily closely as $\tilde{N}_1$ increases. Note, however, that $\lim_{|\tilde{N}_1| \to \infty} \mathbf{b}_1(\tilde{N}_1) \propto \mathbf{v}_1$ would not correlate with the target anymore, so that a proper solution to the SSA problem would not exist, and therefore we must require $\rho_1 < \rho_{max}(L)$ in this case, as claimed. A similar reasoning applies if $w_L = 0$, such that $\rho_1 > -\rho_{max}(L)$. $\square$

Proof of Corollary (4): Let $\gamma_{k+\delta} = \lambda^{k+\delta}$. Then

$$\tilde{b}_k := D\frac{\lambda^\delta}{\lambda^2 - \nu\lambda + 1}\lambda^{k+1} \propto \lambda^{k+\delta} \tag{38}$$

is a solution to

$$\tilde{b}_{k+1} - \nu\tilde{b}_k + \tilde{b}_{k_1} = D\gamma_{k+\delta} , \ 0 \leq k \leq L - 1$$

with boundaries $\tilde{b}_{-1} \neq 0, \tilde{b}_L \approx 0$. The expression is well-defined because $\lambda^2 - \nu\lambda + 1 \neq 0$ since $\lambda \neq \lambda_{\rho_1}$, by assumption. Consider now the solution to the homogeneous difference-equation $db_{k+1} - \nu db_k + db_{k-1} = 0$, namely $db_k = C_1\lambda_{\rho_1}^k + C_2\lambda_{\rho_1}^{L-k}$, where C_1, C_2 are arbitrary constants. We can now combine $\tilde{b}_k$ and db_k as in

$$b_k = b_k(\lambda_{1\rho_1}) \propto \lambda^{k+\delta} + C_1\lambda_{\rho_1}^k + C_2\lambda_{\rho_1}^{L-k} \approx \lambda^{k+\delta} - \lambda_{\rho_1}\lambda^{-1+\delta}\lambda_{\rho_1}^k \tag{39}$$

where we selected $C_1 = -\lambda_{\rho_1}\lambda^{-1+\delta}$, $C_2 = 0$ such that $b_{-1} \approx 0$ and $\tilde{b}_L \approx 0$ (the approximation errors can be neglected by the last assumption of the corollary). Corollary (3) states that the unknown stable root λ_{ρ_1} is determined uniquely by requiring

$$\frac{\sum_{k=1}^{L-1} b_k(\lambda_{\rho_1})b_{k-1}(\lambda_{\rho_1})}{\sum_{k=0}^{L-1} b_k(\lambda_{\rho_1})^2} = \rho_1 \tag{40}$$

We can now insert 39 into this equation and solve for λ_{ρ_1}. Specifically, the nominator becomes

$$\sum_{k=1}^{L-1} b_k b_{k-1} = \sum_{k=1}^{L-1} \left(\lambda^{k+\delta} - \lambda_{\rho_1}\lambda^{-1+\delta}\lambda_{\rho_1}^k\right)\left(\lambda^{k-1+\delta} - \lambda_{\rho_1}\lambda^{-1+\delta}\lambda_{\rho_1}^{k-1}\right) \tag{41}$$

The first cross-product of terms in parantheses is

$$\lambda^{-1}\sum_{k=1}^{L-1} \lambda^{2(k+\delta)} = \lambda^{1+2\delta}\sum_{k=0}^{L-2} \lambda^{2k} = \lambda^{1+2\delta}\frac{1 - \lambda^{2(L-1)}}{1 - \lambda^2} \approx \frac{\lambda^{1+2\delta}}{1 - \lambda^2} \tag{42}$$

The second cross-product of terms in parentheses is

$$-\lambda_{\rho_1}\lambda^{-1+\delta}\sum_{k=1}^{L-1}\lambda^{k+\delta}\lambda_{\rho_1}^{k-1} = -\lambda_{\rho_1}\lambda^{2\delta}\sum_{k=0}^{L-2}(\lambda\lambda_{\rho_1})^k = -\lambda_{\rho_1}\lambda^{2\delta}\frac{1-(\lambda\lambda_{\rho_1})^{L-1}}{1-\lambda\lambda_{\rho_1}} \approx \frac{-\lambda_{\rho_1}\lambda^{2\delta}}{1-\lambda\lambda_{\rho_1}} \quad (43)$$

The third cross-product of terms in parentheses is

$$-\lambda_{\rho_1}\lambda^{-1+\delta}\sum_{k=1}^{L-1}\lambda^{k-1+\delta}\lambda_{\rho_1}^{k} \approx \frac{-\lambda_{\rho_1}^2\lambda^{2\delta-1}}{1-\lambda\lambda_{\rho_1}} \quad (44)$$

The last cross-product of terms in parantheses is

$$\lambda_{\rho_1}^2\lambda^{-2+2\delta}\sum_{k=1}^{L-1}\lambda_{\rho_1}^{2k-1} = \lambda_{\rho_1}^3\lambda^{-2+2\delta}\sum_{k=0}^{L-2}\lambda_{\rho_1}^{2k} = \lambda_{\rho_1}^3\lambda^{-2+2\delta}\frac{1-\lambda_{\rho_1}^{2(L-1)}}{1-\lambda_{\rho_1}^2} \approx \frac{\lambda_{\rho_1}^3\lambda^{-2+2\delta}}{1-\lambda_{\rho_1}^2} \quad (45)$$

The common denominator of 42, 43, 44 and 45 is

$$(1-\lambda^2)(1-\lambda\lambda_{\rho_1})(1-\lambda_{\rho_1}^2) \quad (46)$$

Summing all terms in 42, 43, 44 and 45 under the common denominator 46 leads to a third-order polynomial

$$f_1(\lambda_{\rho_1}) := a_3\lambda_{\rho_1}^3 + a_2\lambda_{\rho_1}^2 + a_1\lambda_{\rho_1} + a_0$$

in λ_{ρ_1} with coefficients $a_3 = \lambda^{2\delta}\lambda^{-2}$, $a_2 = -\lambda^{2\delta}\lambda^{-1}$, $a_1 = -\lambda^{2\delta}$ and $a_0 = \lambda^{2\delta}\lambda$. The coefficient of order four vanishes due to cancellation of cross-terms. The same proceeding can be applied to the denominator $\sum_{k=0}^{L-1}b_k^2$ in 40:

$$\sum_{k=0}^{L-1}b_k^2 \quad = \quad \sum_{k=0}^{L-1}\left(\lambda^{k+\delta}-\lambda_{\rho_1}\lambda^{-1+\delta}\lambda_{\rho_1}^k\right)^2 \quad (47)$$

with cross-products of terms in parentheses

$$\sum_{k=0}^{L-1}\lambda^{2(k+\delta)} \quad \approx \quad \frac{\lambda^{2\delta}}{1-\lambda^2}$$

$$-2\lambda_{\rho_1}\lambda^{2\delta-1}\sum_{k=0}^{L-1}(\lambda\lambda_{\rho_1})^k \quad \approx \quad -\frac{\lambda_{\rho_1}\lambda^{2\delta-1}}{1-\lambda\lambda_{\rho_1}}$$

$$\lambda_{\rho_1}^2\lambda^{-2+2\delta}\sum_{k=0}^{L-1}\lambda_{\rho_1}^{2k} \quad \approx \quad \frac{\lambda_{\rho_1}^2\lambda^{-2+2\delta}}{1-\lambda_{\rho_1}^2}$$

This will lead to the sum of four terms whose common denominator is 46 and whose nominator is a polynomial

$$f_2(\lambda_{\rho_1}) := b_3\lambda_{\rho_1}^3 + b_2\lambda_{\rho_1}^2 + b_1\lambda_{\rho_1} + b_0$$

with polynomial coefficients $b_3 = \lambda^{2\delta}\lambda^{-1}$, $b_2 = \lambda^{2\delta}(\lambda^{-2}-2)$, $b_1 = \lambda^{2\delta}(\lambda-2\lambda^{-1})$ and $b_0 = \lambda^{2\delta}$. After cancelation of their common denominator 46, equation 40 can be re-written as

$$\frac{f_1(\lambda_{\rho_1})}{f_2(\lambda_{\rho_1})} = \rho_1,$$

where the common $\lambda^{2\delta}$ of a_0, a_1, a_2, a_3 and b_0, b_1, b_2, b_3 cancel. We then obtain an equation $f_3(\lambda_{\rho_1}, \rho_1) = 0$ for λ_{ρ_1} where $f_3(\lambda_{\rho_1}, \rho_1)$ is a cubic polynomial in λ_{ρ_1} with coefficients

$$c_3 = \lambda^{-2} - \rho_1\lambda^{-1} \ , \ c_2 = -\lambda^{-1} - \rho_1(\lambda^{-2}-2) \ , \ c_1 = -1 - \rho_1(\lambda-2\lambda^{-1}) \ , \ c_0 = \lambda - \rho_1$$

The remainder of the proof then follows from a closed-form expression for the root of a cubic polynomial (Cardano's formula). Note that $|\rho_1| < 1$ implies $c_3 \neq 0$ so that the solution λ_{ρ_1} to the holding time Equation (40) is the root of a cubic polynomial, as claimed.

Remarks

In contrast to the frequency-domain decomposition 5 of the lag-one autocorrelation, the above time-domain decomposition allows for notable simplifications resulting in a closed-form solution for λ_{ρ_1} under the posited assumptions. Note also that if $|\nu| < 2$ then $\lambda_{1\rho_0}$ is a unit-root so that (some of) the geometric series in the above proof do not converge anymore and therefore high-order terms (of power L) cannot be neglected. The resulting inflated polynomial order is an indication of multiple solutions for ν given ρ_1 in this case. Finally, the solution to Equation (40) in the case of an AR(p) target with $p > 1$ would involve the root of a higher-order polynomial for which a closed-form expression does not exist in general.

9.6 Exact Solution in the Case of Autocorrelation

We derive an exact expression for the SSA predictor in the case of autocorrelated processes. To simplify notation we assume an AR(1)-process for $x_t = a_1 x_{t-1} + \epsilon_t$ but our proceeding is otherwise general. In this case $x_{t-L+j} = \sum_{k=0}^{j-1} \xi_k \epsilon_{t-L+j-k} + \xi_j x_{t-L}$ with $\xi_k = a_1^k$ and therefore

$$y_t = \mathbf{b}_x' \mathbf{x}_t = (\mathbf{\Xi} \mathbf{b}_x)' \boldsymbol{\epsilon}_t + \mathbf{b}_x' \boldsymbol{\xi}_L x_{t-L} = \mathbf{b}_\epsilon' \left(\boldsymbol{\epsilon}_t + \mathbf{\Xi}^{-1\,'} \boldsymbol{\xi}_L x_{t-L} \right) = \mathbf{b}_\epsilon' \left(\boldsymbol{\epsilon}_t + a_1 \mathbf{e}_L x_{t-L} \right), \qquad (48)$$

where $\boldsymbol{\xi}_L := (\xi_L, ..., \xi_1)'$, $\mathbf{e}_L = (0, ..., 0, 1)'$ is a unit vector of length L and the last equality follows from definition of $\mathbf{\Xi}^{-1}$ and $\boldsymbol{\xi}_L$. Factually, the approximation error in (26) originates in the replacement of $b_{xk} x_{t-k}$ by $b_{xk}(\epsilon_{t-k} + \sum_{j=1}^{L-1-k} \psi_j x_{t-k-j})$, where $x_{t-k} = \epsilon_t + \sum_{j \geq 1} \psi_j x_{t-k-j}$ denotes the AR inversion of x_{t-k}. The difference or approximation error $b_{xk} \sum_{j \geq 0} \psi_{L-k+j} x_{t-L-j}$ is attributable to those lags in the AR inversion of x_{t-k} which are not part of the filter: for an AR(1), $\psi_j = \begin{cases} a_1 & j = 1 \\ 0 & j > 1 \end{cases}$ and the rightmost expression in Equation (48) is obtained . We now refer to $\mathbf{b}_\epsilon' \boldsymbol{\epsilon}_t$ and $a_1 \mathbf{e}_L x_{t-L}$ in Equation (48) in terms of main predictor and residual, respectively, and we consider the exact MSE-predictor $y_{t,\epsilon,MSE}$ as applied to $\boldsymbol{\epsilon}_{t\infty} = (\epsilon_t, \epsilon_{t-1}, ...)'$, the semi infinite extension of $\boldsymbol{\epsilon}_t$, with weights $\boldsymbol{\gamma}_{\Xi\delta\infty} := \mathbf{\Xi}_\infty \hat{\boldsymbol{\gamma}}_{x\delta\infty}$ based on the semi-infinite extension of $\mathbf{\Xi}$ applied to $\hat{\boldsymbol{\gamma}}_{x\delta\infty}$ specified by Equation (27). For a derivation of the exact SSA solution, we aim at maximizing the target correlation of y_t with $y_{t,\epsilon,MSE}$ subject to exact length and holding time constraints.

Proposition 3. *Let the above assumptions about x_t and z_t hold. Then the exact finite-length SSA predictor $y_t = \mathbf{b}_x' \mathbf{x}_t = \mathbf{b}_\epsilon' (\boldsymbol{\epsilon}_t + a_1 \mathbf{e}_L x_{t-L})$ is obtained from*

$$\mathbf{b}_\epsilon(\nu_1) = D(\nu_1, l) \tilde{\boldsymbol{\nu}}^{-1} \left(\boldsymbol{\gamma}_{\Xi\delta 1:L} + a_1 \mathbf{e}_L \boldsymbol{\xi}_\infty' \boldsymbol{\gamma}_{\Xi\delta(L+1):\infty} \right), \qquad (49)$$

where the subscripts $1 : L$ and $(L+1) : \infty$ of $\boldsymbol{\gamma}_{\Xi\delta}$ signify corresponding vector entries or lags and where

$$\tilde{\boldsymbol{\nu}} = 2 \left(\mathbf{M} + a_1 \left(1 + \frac{a_1^2}{1 - a_1^2} \right) \mathbf{e}_L \mathbf{e}_L' - \nu_1 \left[\mathbf{I} + \frac{a_1^2}{1 - a_1^2} \mathbf{e}_L \mathbf{e}_L' \right] \right),$$

The pairing $(\nu_1, D(\nu_1, l))$ ensures compliance with holding time and length constraints.

Proof: Noting that $\boldsymbol{\epsilon}_t$ and x_{t-L} are uncorrelated in $y_t = \mathbf{b}_\epsilon' (\boldsymbol{\epsilon}_t + a_1 \mathbf{e}_L x_{t-L})$, the length constraint (unit variance) becomes

$$\mathbf{b}_\epsilon' \left(\mathbf{I} + \frac{a_1^2}{1 - a_1^2} \mathbf{e}_L \mathbf{e}_L' \right) \mathbf{b}_\epsilon = 1, \qquad (50)$$

where $1/(1 - a_1^2) = \sum_{k \geq 0} \xi_k^2$ is the variance or length of x_{t-L}. For the holding time constraint we are looking at the lag-one ACF

$$E\left[\mathbf{b}_\epsilon' \left(\boldsymbol{\epsilon}_t + a_1 \mathbf{e}_L x_{t-L}\right)\left(\boldsymbol{\epsilon}_{t-1} + a_1 \mathbf{e}_L x_{t-1-L}\right)' \mathbf{b}_\epsilon\right],$$

acknowledging that the variance in the denominator of the ACF is unity, due to the length constraint. The above expression becomes

$$\mathbf{b}_\epsilon' \mathbf{M} \mathbf{b}_\epsilon + a_1 \mathbf{b}_\epsilon' \mathbf{e}_L \mathbf{e}_L' \mathbf{b}_\epsilon + \frac{a_1^3}{1 - a_1^2} \mathbf{b}_\epsilon \mathbf{e}_L \mathbf{e}_L' \mathbf{b}_\epsilon, \tag{51}$$

noting that $\boldsymbol{\epsilon}_t$ and x_{t-1-L} are uncorrelated, that $a_1 E[\mathbf{b}_\epsilon' \mathbf{e}_L x_{t-L} \boldsymbol{\epsilon}_{t-1}' \mathbf{b}_\epsilon] = a_1 \mathbf{b}_\epsilon' \mathbf{e}_L \mathbf{e}_L' \mathbf{b}_\epsilon$ and that $a_1^2 E[\mathbf{b}_\epsilon' \mathbf{e}_L x_{t-L} x_{t-1-L} \mathbf{e}_L' \mathbf{b}_\epsilon] = \frac{a_1^3}{1-a_1^2} \mathbf{b}_\epsilon' \mathbf{e}_L \mathbf{e}_L' \mathbf{b}_\epsilon$. We consider next the covariance of the SSA predictor y_t with $y_{t,\epsilon,MSE}$, splitting the task into (mutually independent) residual and main predictor of y_t. The residual $a_1 \mathbf{b}_\epsilon' \mathbf{e}_L x_{t-L}$ correlates with $y_{t,\epsilon,MSE}$ by way of common ϵ_{t-L-k}, $k = 0, 1, ...$ in $x_{t-L} = \boldsymbol{\xi}_\infty' \boldsymbol{\epsilon}_{t-L\infty}$ and $\boldsymbol{\gamma}_{\Xi\delta\infty} \boldsymbol{\epsilon}_{t\infty}$. Aggregating over common terms we obtain $a_1 \mathbf{b}_\epsilon' \mathbf{e}_L \boldsymbol{\xi}_\infty' \boldsymbol{\gamma}_{\Xi\delta(L+1):\infty}$ for the residual covariance. Similarly, the covariance between the main predictor $\mathbf{b}_\epsilon' \boldsymbol{\epsilon}_t$ and $\boldsymbol{\gamma}_{\Xi\delta\infty} \boldsymbol{\epsilon}_{t,\infty}$ is $\mathbf{b}_\epsilon' \boldsymbol{\gamma}_{\Xi\delta 1:L}$. Summing both contributions we obtain

$$E[y_t y_{t,\epsilon,MSE}] = \mathbf{b}_\epsilon' \left(\boldsymbol{\gamma}_{\Xi\delta 1:L} + a_1 \mathbf{e}_L \boldsymbol{\xi}_\infty' \boldsymbol{\gamma}_{\Xi\delta(L+1):\infty}\right) \tag{52}$$

for the covariance of y_t and $y_{t,\epsilon,MSE}$. If the length constraint (50) is imposed, then the covariance (52) is proportional to the target correlation and therefore we can proceed to optimization, maximizing (52) subject to (50) and (51). Taking derivatives of the Lagrangian then leads to a system of equations for $\mathbf{b}_\epsilon$

$$2\tilde{\lambda}_2 \left\{ \mathbf{M} + a_1 \left(1 + \frac{a_1^2}{1 - a_1^2}\right) \mathbf{e}_L \mathbf{e}_L' \right\} \mathbf{b}_\epsilon + 2\tilde{\lambda}_1 \left[\mathbf{I} + \frac{a_1^2}{1 - a_1^2} \mathbf{e}_L \mathbf{e}_L'\right] \mathbf{b}_\epsilon$$
$$= \boldsymbol{\gamma}_{\Xi\delta 1:L} + a_1 \mathbf{e}_L \boldsymbol{\xi}_\infty' \boldsymbol{\gamma}_{\Xi\delta(L+1):\infty}$$

from which Equation (49) can be inferred. The resulting solution maximizes the correlation with the exact (infinite length) MSE-predictor, up to a fixed scaling constant and subject to exact lag-one and length constraints and therefore $y_t = \mathbf{b}_x' \mathbf{x}_t = \mathbf{b}_\epsilon' \left(\boldsymbol{\epsilon}_t + a_1 \mathbf{e}_L x_{t-L}\right)$ can be interpreted as (exact) SSA predictor, as claimed. $\qquad \square$

Remarks: in principle, the above proof can be extended to arbitrary stationary or integrated (invertible) processes but the correction terms will be more complex than for the considered AR(1) process, thus cluttering the notation correspondingly. In general, ξ_k and ϵ_j are unknown and must be estimated: we refer to textbooks on the topic, see Brockwell and Davis (1993). Wildi (2024) shows that the impact of the finite sample estimation error remains negligible for practical sample sizes ($T = 120$ observations corresponding to 10 years of monthly data), assuming the lag-one autocorrelation is not too large; specifically, values smaller than 0.9 in absolute value help mitigate finite sample biases and outliers of the holding time. In any case, we may refer to our SSA package for a quantification of corresponding effects.

9.7 SSA Optimization for I(2) Processes

Processes of integration order two are important insofar that some well-known designs, such as the HP-filter, can be derived by relying on a corresponding smooth trend model assumption, see Harvey (1989). Let then z_t and $\tilde{x}_t$ be both I(2) so that $y_{t,MSE\infty}$ specified by Equation (29) is I(2) and $p(t) = \tilde{x}_0 + (\tilde{x}_1 - \tilde{x}_0)t$ is a linear time trend. We can then exchange the proper target by the MSE-predictor in the SSA criterion and the cointegration constraints can be splitted into a level constraint $\sum_{k=0}^{L-1} b_{\tilde{x}k} = \Gamma(0)$ and a slope constraint $\sum_{k>0} b_{\tilde{x}k} k = \dot{\Gamma}(0)$, where $\dot{\Gamma}(0)$ denotes the

derivative of the transfer function (of either target or MSE filters). We denote by $y_{t,MSE}$, with coefficients $\hat{\boldsymbol{\gamma}}_{MSE;L}$, the finite length MSE filter, subject to the same cointegration constraints: as for the previous I(1) case, an exact specification of the latter filter is not explicitly required. A cancellation of the double unit-root by the error filter $e_t = y_{t,MSE} - y_t$ is then obtained from

$$y_{t,MSE} - y_t \;=\; (\hat{\boldsymbol{\gamma}}_{MSE,L} - \mathbf{b}_{\tilde{x}})'\tilde{\mathbf{x}}_t = (\hat{\boldsymbol{\gamma}}_{MSE,L} - \mathbf{b}_{\tilde{x}})'\boldsymbol{\Sigma}^2{}'\boldsymbol{\Delta}^2{}'\tilde{\mathbf{x}}_t = (\hat{\boldsymbol{\gamma}}_{MSE,L} - \mathbf{b}_{\tilde{x}})'\boldsymbol{\Sigma}^2{}'\mathbf{x}_t \tag{53}$$

where the first $L-2$ entries of $\boldsymbol{\Delta}^2{}'\tilde{\mathbf{x}}_t$ are the stationary second order differences $x_t, x_{t-1}, ..., x_{t-(L-3)}$ and where we substitued $x_{t-(L-2)}, x_{t-(L-1)}$ for the last two non-stationary entries of the vector. This subsitution is legitimate because the last two columns of $\boldsymbol{\Sigma}^2{}'$ are $(L-1-k)_{k=0,...,L-1}$ and $(L-k)_{k=0,...,L-1}$, respectively: the level constraint cancels the constants $L-1$ and L of each column and the slope constraint cancels the linear trend $(-k)_{k=0,...,L-1}$. Therefore, the last two entries of $(\hat{\boldsymbol{\gamma}}_{MSE,L} - \mathbf{b}_{\tilde{x}})'\boldsymbol{\Sigma}^2{}'$ vanish so that the above identity applies. In the next step, we want to replace $\mathbf{x}_t$ by the finite MA-inversion $\boldsymbol{\Xi}'\boldsymbol{\epsilon}_t$ in Equation (53). For this purpose, we rely on $\sum_{k=0}^{L-1}|b_{\tilde{x},k}k^2| < N$, $\sum_{k=0}^{L-1}|\hat{\gamma}_{MSE,k}k^2| < N$ for all L and we use the same argument as in the I(1) case, to infer that $(\hat{\boldsymbol{\gamma}}_{MSE,L} - \mathbf{b}_{\tilde{x}})'\boldsymbol{\Sigma}^2{}'$ is absolutely summable so that the filter error is stationary with spectral density $\left|\boldsymbol{\Sigma}^2(\hat{\boldsymbol{\gamma}}_{MSE,L} - \mathbf{b}_{\tilde{x}})\right|^2(\omega)h_x(\omega)$. Then, the finite MA-approximation is pertinent, assuming sufficiently fast decaying ξ_k. The two equivalent SSA optimization criteria are then obtained from Equation (32), substituting $\boldsymbol{\Sigma}^2{}'$ for $\boldsymbol{\Sigma}'$

$$\left.\begin{array}{c} \max_{\mathbf{b}_\epsilon} \mathbf{b}_\epsilon'\boldsymbol{\Sigma}^2{}'\boldsymbol{\gamma}_{\tilde{\Xi}\delta} \\ \mathbf{b}_\epsilon'\mathbf{M}\mathbf{b}_\epsilon = \rho_1\mathbf{b}_\epsilon'\mathbf{b}_\epsilon \\ \mathbf{b}_\epsilon'\boldsymbol{\Sigma}^2{}'\boldsymbol{\Sigma}^2\mathbf{b}_\epsilon = l \end{array}\right\} \quad \text{or} \quad \left.\begin{array}{c} \min_{\mathbf{b}_\epsilon}(\boldsymbol{\gamma}_{\tilde{\Xi}\delta} - \boldsymbol{\Sigma}^2\mathbf{b}_\epsilon)'(\boldsymbol{\gamma}_{\tilde{\Xi}\delta} - \boldsymbol{\Sigma}^2\mathbf{b}_\epsilon) \\ \mathbf{b}_\epsilon'\mathbf{M}\mathbf{b}_\epsilon = \rho_1\mathbf{b}_\epsilon'\mathbf{b}_\epsilon \end{array}\right\}.$$

where $\boldsymbol{\gamma}_{\tilde{\Xi}\delta} = \boldsymbol{\Sigma}^2\boldsymbol{\Xi}\hat{\gamma}_{MSE,L}$. In a final step, we can implement level and slope constraints: solving for $b_{\tilde{x}0}, b_{\tilde{x}1}$ we obtain $\mathbf{b}_{\tilde{x}} = (\Gamma(0) - \dot{\Gamma}(0))\mathbf{e}_1 + \dot{\Gamma}(0)\mathbf{e}_2 + \mathbf{B}\tilde{\mathbf{b}}$, where $\tilde{\mathbf{b}}$ is a vector of free parameters of length $L-2$ and $\mathbf{B}$ is an $L \cdot (L-2)$ dimensional matrix whose first two rows are $(k)_{k=1,...,L-2}$ and $(-k)_{k=2,...,L-1}$ and the remaining $L-2$ rows correspond to an identity. An extension of Equation (33) is then straightforward, but is skipped here for simplicity of exposition.

References

[1] Anderson O.D. (1975) Moving Average Processes. *Journal of the Royal Statistical Society. Series D (The Statistician)*. **Vol. 24, No. 4**, 283-297

[2] Barnett J.T. (1996) Zero-crossing rates of some non-Gaussian processes with application to detection and estimation. *Thesis report Ph.D.96-10, University of Maryland.*

[3] Baxter, M. and R.G. King (1999). Measuring business cycles: Approximate band-pass filters for economic time series. *Review of Economics and Statistics* **81**, 575–593.

[4] Brockwell P.J. and Davis R.A. (1993) Time Series: Theories and Methods (second edition). *Springer Verlag.*

[5] Davies, N., Pate, M. B. and Frost, M. G. (1974). Maximum autocorrelations for moving average processes. *Biometrika* **61**, 199-200.

[6] Hamilton, J.D. (2018). Why you should never use the Hodrick-Prescott filter. *Review of Economics and Statistics* **100**, 831–843.

[7] Harvey, A. (1989). Forecasting, structural time series models and the Kalman filter. *Cambridge: Cambridge University Press.*

[8] Henderson, R. (1924). A New Method of Graduation. *Transactions of the Actuarial Society of America* **25**, 29–40

[9] Hodrick, R. and Prescott, E. (1997) Postwar U.S. business cycles: an empirical investigation. *Journal of Money, Credit, and Banking* **29**, 1–16.

[10] Kedem, B. (1986) Zero-crossings analysis. *Research report AFOSR-TR-86-0413, Univ. of Maryland.*

[11] Kratz, M. (2006) Level crossings and other level functionals of stationary Gaussian processes. *Probability surveys* **Vol. 3**, 230-288.

[12] McElroy, T. (2008) Matrix formulas for nonstationary ARIMA signal extraction. *Econometric Theory* **24**, 1—22.

[13] McElroy, T. and Wildi , M. (2019) The trilemma between accuracy, timeliness and smoothness in real-time signal extraction. *International Journal of Forecasting* **35 (3)**, 1072-1084.

[14] McElroy, T. and Wildi , M. (2020) The multivariate linear prediction problem: model-based and direct filtering solutions. *Econometrics and Statistics* **14**, 112-130.

[15] Rice,S.O. (1944) Mathematical analysis of random noise. *I. Bell. Syst. Tech. J* **23**, 282-332.

[16] Whittaker, E.T. (1922). On a New Method of Graduation. *Proceedings of the Edinburgh Mathematical Society* , **41** , 63 - 75.

[17] Wildi, M. (2024) Business-Cycle Analysis and Zero-Crossings of Time Series: a Generalized Forecast Approach. Submitted for publication to the Journal of Business Cycle Analysis.